

# AGMARL-DKS: An Adaptive Graph-Enhanced Multi-Agent Reinforcement Learning for Dynamic Kubernetes Scheduling

Hamed Hamzeh<sup>1\*</sup>

<sup>1</sup>Computer Science and Engineering, University of Westminster, 115 New Cavendish Street, London, W1W 6UW, United Kingdom.

Corresponding author(s). E-mail(s): [H.Hamzeh@westminster.ac.uk](mailto:H.Hamzeh@westminster.ac.uk);

## Abstract

State-of-the-art cloud-native applications require intelligent schedulers that can effectively balance system stability, resource utilisation, and associated costs. While Kubernetes provides feasibility-based placement by default, recent research efforts have explored the use of reinforcement learning (RL) for more intelligent scheduling decisions. However, current RL-based schedulers have three major limitations. First, most of these schedulers use monolithic centralised agents, which are non-scalable for large heterogeneous clusters. Second, the ones that use multi-objective reward functions assume simple, static, linear combinations of the objectives. Third, no previous work has produced a stress-aware scheduler that can react adaptively to dynamic conditions. To address these gaps in current research, we propose the Adaptive Graph-enhanced Multi-Agent Reinforcement Learning Dynamic Kubernetes Scheduler (AGMARL-DKS). AGMARL-DKS addresses these gaps by introducing three major innovations. First, we construct a scalable solution by treating the scheduling challenge as a cooperative multi-agent problem, where every cluster node operates as an agent, employing centralised training methods before decentralised execution. Second, to be context-aware and yet decentralised, we use a Graph Neural Network (GNN) to build a state representation of the global cluster context at each agent. This represents an improvement over methods that rely solely on local observations. Finally, to make trade-offs between these objectives, we use a stress-aware lexicographical ordering policy instead of a simple, static linear weighting of these objectives. The evaluations in Google Kubernetes Engine (GKE) reveal that AGMARL-DKS significantly outperforms the default scheduler in terms of fault tolerance, utilisation, and cost, especially in scheduling batch and mission-critical workloads.

**Keywords:** Fault Tolerance, Graph Neural Networks (GNNs), Kubernetes Scheduling, Lexicographical Optimization, Multi-Agent Reinforcement Learning (MARL), Stress-Aware Systems

## 1 Introduction

Kubernetes is the de facto standard open-source container orchestration platform for large-scale, distributed applications [1, 2]. The core concept in Kubernetes is the *pod*, which is an instance of a running process that holds one or more containers for tightly coupled workloads [3]. Assigning a pod to a node in the cluster is a multi-dimensional optimisation problem [6]. Practical pod placement needs to account dynamically and simultaneously for a large set of continuously changing parameters, including highly heterogeneous workloads, node capabilities, resource requirements, and constraints, as well as competing deployment objectives (e.g., load balancing, resource utilisation) [4]. Pod placement quality is therefore a fundamentally important problem with a direct impact on the system’s stability, resource utilisation, cost and responsiveness [5]. The built-in default scheduler of Kubernetes employs feasibility-based pod placement, which proves too basic for handling real-world complex environments since it evaluates only basic node resource availability for hosting pods [7]. Significant work has been done to integrate complex heuristics and specialised algorithms into Kubernetes systems, but these solutions introduce trade-offs with operational concerns and system complexity [4, 10]. The present solutions target specific workloads, but their specialisation leads to performance improvements theoretically while substantially increasing operational complexity and system maintenance requirements. Critically, this category of solutions also suffers from a fundamental set of scalability and adaptability problems in dynamic, heterogeneous workloads, which makes them brittle and unresponsive to shifting application requirements [4, 10, 11].

To overcome the challenges of fixed heuristics, recent works have begun to focus on developing more intelligent and adaptive frameworks based on Reinforcement Learning (RL) [8, 12, 20, 21, 31]. However, since today’s cloud cluster scenarios are more complex and the state space is high-dimensional, it is necessary to introduce Deep Reinforcement Learning (DRL) with deep neural networks to represent the value and policy functions [29]. The key idea of DRL is to treat the Kubernetes scheduler as a DRL agent that can learn a generalisable placement policy by interacting with the environment [12, 21, 23, 25, 31, 31–38]. The agent receives observations about the current system state, such as node resource utilisation, workload requirements, and network bandwidth, and produces actions through the scheduler to improve performance using a reward signal as a learning guide. In this way, the agent can identify complex non-linear scheduling policies from raw data. In addition, this data-driven approach also provides a means for schedulers to learn highly customised policies to adapt to various real-world deployment environments, compared to the general-purpose algorithmic framework. For example, a Dynamic Resource Scheduling (DRS) framework formulates the Kubernetes scheduling problem as a Markov decision process and applies DRL to significantly improve the load balancing and optimisation [8].

However, traditional single-agent DRL frameworks are ill-suited to large-scale environments. Monolithic centralised agents restrict scalability in large clusters due to the exponential growth of state and action dimensions [7, 13]. Centralized single-agent decisions demonstrate slow response times [12], form a point of failure, and lack global optimality [18, 19]. An intuitive alternative is a multi-agent (MARL) approach [14]. MARL uses multiple, local agents (one per node), providing natural scalability and fault tolerance [30]. The approach presents specific challenges which primarily involve coordinating multiple agents [15]. In addition, previous RL schedulers, even MARL, do not adequately account for other important limitations. Scheduling is a multi-objective problem that combines potentially competing metrics (fault tolerance, utilisation, cost) [9, 16, 22]. The complex nature of dynamic Kubernetes environments led previous studies to adopt static linear reward combinations that failed to reflect non-linear and state-dependent priorities [12, 17, 21]. None of the previous research offers explicit "stress-aware" capability which would allow policies to adapt dynamically to emerging cluster stress. Effective intelligent scheduling thus requires not only coordination, but dynamic multi-objective management and stress-awareness.

To overcome these limitations, we present the Adaptive Graph-enhanced Multi-Agent Reinforcement Learning Dynamic Kubernetes Scheduler (AGMARL-DKS). The framework adopts MADD4PG [24, 28] as the foundational model and transforms scheduling into a collaborative process where each cluster node acts as an independent agent. The design permits a scalable and decentralised system [25, 26] yet presents difficulties in synchronising local decisions with overarching objectives. AGMARL-DKS addresses this with a Centralised Training with Decentralised Execution (CTDE) framework [58]. A centralised critic utilises global information to train decentralised agents throughout the offline phase which solves the non-stationarity challenge present in multi-agent systems [27]. The online phase enables each agent to independently and immediately use GNN-augmented local observations for decision-making. The model adopts a hierarchical structure of metrics to optimally trade off between fault tolerance, resource utilisation and cost.

The primary contributions of this research can be summarised as follows:

1. By prioritising scheduling decisions according to a predetermined order of fault tolerance, resource utilisation, and cost, a lexicographic ordering technique more successfully handles the multi-objective nature of pod placement than current approaches.
2. A multi-agent architecture that alleviates complexity issues, improves scalability in large Kubernetes clusters, and allows decentralised decision-making.
3. Graph Neural Networks (GNNs) are integrated to provide each agent with a context-rich local observation of the entire cluster state, enabling sophisticated coordination without direct communication.
4. A novel hybrid policy that combines learned, multi-objective evaluations from decentralised actors with a centralised, stress-aware lexicographical selection mechanism, allowing agents to learn what is important while the system dictates how to prioritise it.

5. The algorithm may dynamically modify its behaviour depending on the current cluster circumstances thanks to an adaptive learning rate mechanism and a stress-aware reward function, meeting the demand for flexibility in a variety of dynamic situations.
6. We compare the performance of AGMARL-DKS with baseline Kubernetes scheduler on the production-grade Google Kubernetes Engine (GKE) under two comprehensive, custom-designed stress-test scenarios. We show that AGMARL-DKS learns an intelligent smart consolidation policy for resource-intensive workloads, and an strategic self-restraint policy to preserve system stability under churn and fault-injection. Most notably, our correlation analysis gives direct evidence that AGMARL-DKS can successfully decouple conflicting goals of fault tolerance and resource utilisation as a fundamental limitation of existing schedulers, through learning a sophisticated, risk-aware policy.

The remaining paper has been organised as follows. Section 3 discusses the problem statement, including AGMARL-DKS formulation. Section 4 explains the experimental setup and how the workload is generated for evaluation. Section 5 contains the assessment and results. Finally, in section 6, we discuss the conclusion.

## 2 Related Work

Recent works have started to explore the use of Deep Reinforcement Learning (DRL) for cloud and fog computing scheduling. The proposed new approach shows potential to solve critical limitations of static heuristic methods like scalability problems and true multi-objective optimisation gaps while also improving adaptation to changing cluster stress levels.

In [31], the authors use the combination of deep and reinforcement learning to adaptively schedule tasks in order to increase resource utilisation. This method does result in increased efficiency; however, this solution almost always uses a single monolithic agent with a very simple and static combination of rewards. We take a step further with AGMARL-DKS by developing a scalable multi-agent system and a stress-aware lexicographical ordering policy. The work in [32] proposes DRL4HFC, a multi-agent DRL model for microservices placement in Fog/Cloud environments. It successfully minimizes execution time and resource consumption, but the need for manual parameter fine-tuning of DRL agents makes it unsuitable for dynamic and heterogeneous Kubernetes clusters. In contrast, AGMARL-DKS uses an adaptive learning mechanism that can automatically adjust to varying cluster configurations.

Other approaches have been proposed for fog and IoT environments, such as the Dynamic Mayfly Optimisation Scheduling (DMOS) algorithm [33] which is aimed towards energy efficiency and reliability. This paper’s approach is fog-specific to task scheduling and it does not consider the intricacies of Kubernetes pod placement. AGMARL-DKS is Kubernetes-specific as a scheduler, aiming to solve challenges of container orchestration such as resource pressures and pod-to-node constraints.

Decentralised agent-based architectures, e.g. The work presented in [34] demonstrates superior resilience to fog system failures but confines agent decision-making

to local data sources which diminishes global decision effectiveness. The AGMARL-DKS method delivers improved functionality compared to previous approaches by developing Graph Neural Networks (GNNs) utilising a Centralised Training with Decentralised Execution (CTDE) model. This yields each agent an observation embedding of the entire cluster state, endowing it with context to support complex coordination.

A decentralised scheduling solution based on a Spatial Prisoner’s Dilemma game-theoretic model is proposed in [35]. The proposed approach is scalable, but its direct application to the problem is limited due to its reliance on cellular automata and a particular game model. The state space of Kubernetes, on the other hand, is far more complex and dynamic. AGMARL-DKS overcomes these limitations by implementing a flexible multi-agent DRL approach that learns the policies through direct interaction with the environment.

The Hierarchical Multi-Agent Optimisation (HMAO) algorithm [36] also applies a multi-agent approach to resource utilisation optimisation. This aspect is not a novelty in comparison to our work, but HMAO does not provide a method for the agents to dynamically perceive the global state. AGMARL-DKS builds on this concept by implementing GNNs to facilitate dynamic sharing of comprehensive cluster topology and health representations among agents.

Approaches based on single-agent DRL have also been explored, such as the Deep Q-Network (DQN) based model for workflow scheduling in [37] and the RL-based Kubernetes plugin RLKube [21]. RLKube for example outperforms the default scheduler in terms of throughput and energy efficiency. Monolithic single-agent architectures at their core fail to scale effectively within the complex high-dimensional state space found in extensive clusters. By contrast, AGMARL-DKS is intrinsically more scalable and robust as it distributes intelligence (one agent per node).

In the context of our work, a recent and very related contribution [25] is a multi-agent DRL framework for container allocation. The approach provides confirmation of the benefit of a multi-agent modelling approach. Although this work combined with [37] exhibits reinforcement learning potential they fail to model and prioritize competing objectives during stress conditions unlike AGMARL-DKS which handles these situations effectively. The system lacks both formal lexicographical ordering and stress-aware properties which are critical for AGMARL-DKS to enable principled decisions during state-dependent conflicts.

Our research shares significant similarities with the concurrent work in [38] as both studies employ Graph Neural Networks (GIN) for multi-objective application placement tasks. This work essentially validates our choice to use a GNN to model the dependencies, however they still use a standard actor-critic architecture to implicitly learn the trade-offs. In contrast, AGMARL-DKS marries the GNN based state representation with an \*explicit\* stress-aware lexicographical policy. This hybrid approach not only allows agents to learn what constitutes a good placement, but the policy also allows the system to control how to prioritise between placements in terms of the overall system stress, in an interpretable and controllable way.

Approach	Lexicographic Ordering	Adaptive Learning	Graph Neural Networks	Multi-agent System	Kubernetes-specific	Fault Tolerance	Energy Efficiency	Decentralized Architecture	Scalability	Stress-aware
AGMARL-DKS	✓	✓	✓	✓	✓	✓	✓	✓	✓	✓
DRL4HFC	-	✓	-	✓	-	-	✓	-	✓	-
DMOS	-	✓	-	-	-	✓	✓	✓	-	-
Game Theoretic	-	-	-	✓	-	✓	-	✓	✓	-
HMAO	-	-	-	✓	-	-	✓	✓	✓	-
RLKube	-	✓	-	-	✓	-	✓	-	✓	-
DRL-GIN	-	✓	✓	-	-	-	-	-	✓	-
DRL Framework	-	✓	-	-	-	-	-	-	✓	-
Multi-agent DRL	-	✓	-	✓	✓	-	-	✓	✓	-
Agent-based Framework	-	-	-	✓	-	✓	-	✓	✓	-

**Table 1:** Comprehensive Feature Comparison of Different Approaches

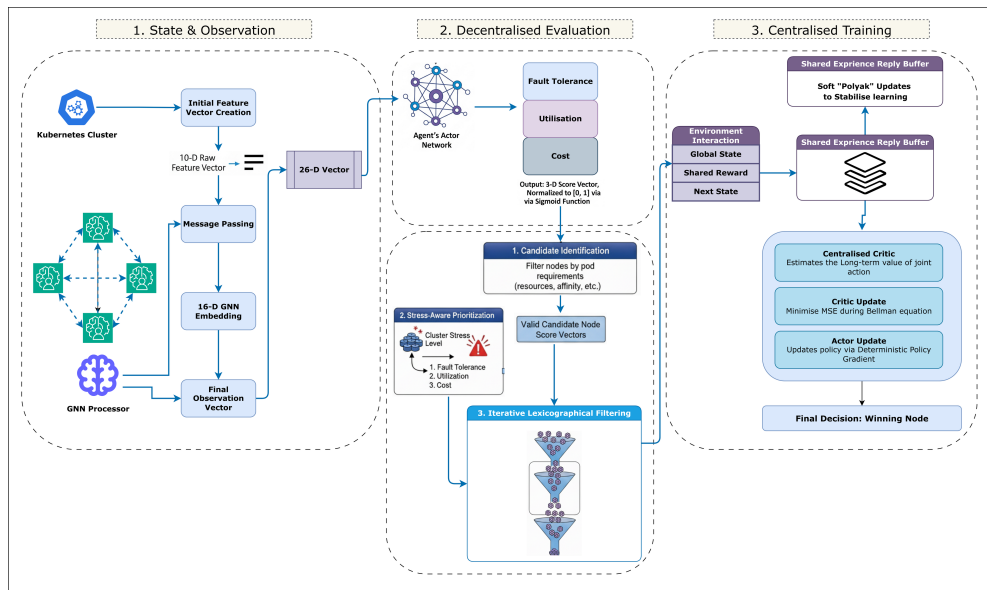


**Fig. 1:** AGMARL-DKS development Pipeline

### 3 Approach

The AGMARL-DKS approach is designed to handle the dynamic multi-objective nature of pod scheduling in Kubernetes environments by utilising a cooperative multi-agent reinforcement learning framework [39]. The pod scheduling problem is formulated as a partially observable multi-agent MDP, with the objective of learning a joint policy that achieves global system objectives [40]. This method departs from a traditional centralised and monolithic scheduler approach by distributing intelligence across decentralised, autonomous agents. By adopting a centralised training and decentralised execution approach, complex coordination strategies can be learned offline, while still supporting fast and scalable online decision-making [58].

#### 3.1 Problem Formulation as a Multi-Agent System

Our solution models the pod scheduling decision-making process as a fully cooperative *multi-agent Markov decision process* (MAMDP) [41]. The use of MAMDPs is natural in this setting because they are a mathematical formalism that naturally captures the interaction of the set of distributed cooperative agents; one per Kubernetes node in our system. An MAMDP is given by:

$$\mathcal{M} = \langle \mathcal{S}, \{\mathcal{O}_i\}_{i=1}^N, \{\mathcal{A}_i\}_{i=1}^N, \mathcal{P}, \mathcal{R}, \gamma \rangle \quad (1)$$

where the components are defined as follows:

- $\mathcal{S}$  is the global state space, representing the collective state of the entire Kubernetes cluster at any given time.
- $\{\mathcal{O}_i\}_{i=1}^N$  is the set of observation spaces. Each agent  $i$  perceives the environment through its own local observation  $o_i \in \mathcal{O}_i$ .
- $\{\mathcal{A}_i\}_{i=1}^N$  is the set of action spaces. Each agent  $i$  can take an action  $a_i \in \mathcal{A}_i$ .
- $\mathcal{P} : \mathcal{S} \times \mathcal{A}_1 \times \dots \times \mathcal{A}_N \times \mathcal{S} \rightarrow [0, 1]$  is the state transition probability function, which defines the dynamics of the environment based on the joint action of all agents.
- $\mathcal{R} : \mathcal{S} \times \mathcal{A}_1 \times \dots \times \mathcal{A}_N \rightarrow \mathbb{R}$  is the shared reward function, which provides a global feedback signal to all agents for their collective behaviour.
- $\gamma \in [0, 1)$  is the discount factor, which balances the importance of immediate versus future rewards.

Each component of this tuple is instantiated to capture the specific dynamics and requirements of the Kubernetes scheduling problem within the *AGMARL-DKS* framework, as detailed in the following paragraphs.

##### *State and Observations*

The global state of the environment  $s_t \in \mathcal{S}$  at the point of scheduling event  $t$  is a representation of the current configuration of the full Kubernetes cluster. In our model, this is a graph  $s_t = \mathcal{G}_t = (V, E)$ , where  $V$  are worker nodes in the cluster, and  $E$  are edges between them. For each node  $i \in V$  there is a raw feature vector of dimension 10,  $x_{i,t} \in \mathbb{R}^{10}$ , that describes its local state. This consists of the current allocations for CPU and memory as well as other health and performance metrics, such as a binary indicator for `MemoryPressure` and the number of pod restarts in the last hour. While

the true state  $s_t$  is global, in accordance with the principle of decentralised execution, each agent  $i$  acts based on a local observation,  $o_{i,t} \in \mathcal{O}_i$ . A distinguishing feature of our approach is that this is not a naive local observation but is instead augmented with global context. Accordingly, we concatenate the agents 10-dimensional raw local metrics with a 16-dimensional dense embedding,  $e_{i,t}$ , generated by a shared GNN [43] from the full cluster graph.

This GNN thus accepts the entire cluster graph  $\mathcal{G}_t$  as input and, through a number of message passing steps, computes an embedding  $e_{i,t}$  for each node, capturing high-order information about the global topology and state of the entire cluster into a fixed-size vector. The complete 26-dimensional local observation for each agent  $i$  is then given by:

$$o_{i,t} = \text{concat}(x_{i,t}, e_{i,t})$$

This design facilitates the propagation of the GNN embedding into each agent’s local observation, in order to diffuse global context to every agent’s local perception. In this way, agents can make globally-aware decisions that implicitly consider the state of the entire system, enabling high-level coordination without requiring agent-to-agent communication at execution time.

### ***Actions***

The action space of agent  $i$ , denoted as  $\mathcal{A}_i$ , is a continuous 3 dimensional vector space,  $\mathcal{A}_i \subseteq \mathbb{R}^3$ . The action  $a_{i,t} \in \mathcal{A}_i$  is not an actual control command (e.g. ”accept pod”) but a learned, multi-objective, ranking of the suitability of its own node for the pending pod. The action vector  $a_{i,t} = [\text{score}_{\text{FT}}, \text{score}_{\text{UTIL}}, \text{score}_{\text{COST}}]$  is the output of agent  $i$ ’s deterministic actor network,  $\mu_{\theta_i}$ , in which the logits of the final layer are run through a sigmoid activation to bound the scores to the range  $(0, 1)$ . The larger the score, the greater the belief of the agent that placing the pod on its node will result in a desirable outcome for that objective. The metrics that underlie these learned scores are defined below.

*Fault Tolerance ( $\text{score}_{\text{FT}}$ ).* This metric measures a node’s stability and trustworthiness. It has two parts: the past stability of the node, and its current health. Let  $R_i$  be the number of pod restarts on node  $i$  over a recent time window, and let  $H_i \in \{0, 1\}$  be a binary flag indicating that a node is currently under some kind of pressure (e.g. `MemoryPressure`). Let  $H_i = 1$  represent an unhealthy node. We define the fault tolerance metric  $M_{\text{FT},i}$  of node  $i$  as:

$$M_{\text{FT},i} = (1 - H_i) \cdot \frac{1}{1 + \log(1 + R_i)} \quad (2)$$

The  $(1 - H_i)$  term is a hard constraint. If the node is under active pressure, the score becomes zero and that node is immediately eliminated from contention. For healthy nodes, the score scales inversely to the logarithm of the restart count. The logarithm function serves to reduce extreme restart count outliers’ effect to prevent the metric from being excessively skewed by the worst performing node but retains sensitivity to initial instability signs.

*Resource Utilization (score<sub>UTIL</sub>).* This score should incentivize efficient packing (consolidation) without overloading the nodes. Placements are rewarded on nodes that already have a high utilization. Here  $C_i^{\text{alloc}}$  and  $M_i^{\text{alloc}}$  are the allocated CPU and memory on node  $i$ , while  $C_i^{\text{cap}}$  and  $M_i^{\text{cap}}$  are the capacity of these resources. The resulting utilization metric,  $M_{\text{UTIL},i}$ , is the average of the utilization of both:

$$M_{\text{UTIL},i} = \frac{1}{2} \left( \frac{C_i^{\text{alloc}}}{C_i^{\text{cap}}} + \frac{M_i^{\text{alloc}}}{M_i^{\text{cap}}} \right) \quad (3)$$

Ideally, the agent’s policy should learn to assign a high score<sub>UTIL</sub> to nodes where the value is high but not necessarily critical, essentially learning a ”packing” strategy. The GNN-enhanced observation allows the agent to decide if packing on its node is globally optimal.

*Cost Efficiency (score<sub>COST</sub>).* This score measures the economic cost of scheduling a pod on a particular node. This is dependent on the instance type in a cloud setting (general-purpose, memory-optimised, spot etc). Let  $\text{Cost}_i$  be the normalised hourly cost of the instance type for node  $i$ . The cost efficiency metric is then:

$$M_{\text{COST},i} = \frac{1}{\text{Cost}_i} \quad (4)$$

This objective formulation incentivizes nodes with lower cost to be more efficient. The agent’s actor network learns to output a high score<sub>COST</sub> that it’s own node is an economical favorable option compared to other available nodes.

### *Policy and State Transitions*

The algorithm used in the framework is based on a hybrid policy,  $\pi$ , consisting of the decentralised roll-out value estimation from the agents’ local actors, as well as a centralised, deterministic placement logic which makes the final action selection [42, 44]. This hybrid policy can be factorised into:

1. **Decentralised Score Generation:** At each scheduling event  $t$ , every agent  $i$  in the candidate set  $\mathcal{C}_t$  applies its learned actor policy  $\mu_{\theta_i}$  to its local observation  $o_{i,t}$ . This produces a vector of objective scores,  $a_{i,t}$ . The collection of these scores from all candidate agents forms the joint action set:

$$\mathbf{a}_t = \{a_{i,t} \mid i \in \mathcal{C}_t\} = \{\mu_{\theta_i}(o_{i,t}) \mid i \in \mathcal{C}_t\}$$

2. **Centralised Node Selection:** A central controller then applies a high-level, deterministic policy function,  $\Lambda$ . This function implements the stress-aware lexicographical filtering algorithm [45], taking the joint action set  $\mathbf{a}_t$  and the current global stress level  $L_t$  as input to select the single winning node,  $i^*$ :

$$i^* = \Lambda(\mathbf{a}_t, L_t)$$

The state transition function  $\mathcal{P}(s_{t+1} \mid s_t, i^*)$  is then implicitly performed by the Kubernetes control plane. The winning node  $i^*$  selecting a binding action is performed by `kube-apiserver` as state updates to the cluster’s resource allocations and other

state variables to transition from  $s_t$  to  $s_{t+1}$ . The internals of Kubernetes’ operation are a complex subject on their own, but under our model, this occurs as a deterministic environment transition due to the selection of  $i^*$ . The hybrid approach cleanly separates the learning of complex value estimations involving decentralised actors from executing high-level strategic priorities based on centralised logic [44].

### **Reward**

The agents operate under a collective reward function  $\mathcal{R}(s, \mathbf{a})$  which exists to promote joint cooperative behavior. Rather than having each agent compete against the others, the collection of agents as a system are intended to learn a joint policy for system-wide optimisation [46].

A global reward signal  $R_t$  is computed after the placement decision is applied to the winning node  $i^*$ . The reward is designed to incentivise the agents to learn to be accurate estimators of their own fitness for the placement task. In order to compute the reward, we first observe the vector of true, post-placement metric values at the winning node:  $m_t^* = [m_{\text{FT}}^*, m_{\text{UTIL}}^*, m_{\text{COST}}^*]$ , the ground-truth values of fault tolerance, utilisation, and cost efficiency, respectively, that are achieved as a result of the placement.

The global reward  $R_t$  is then formulated as:

$$R_t = -\frac{1}{3} \sum_{j=1}^3 (a_{i^*,t,j} - m_{t,j}^*)^2 + B$$

This function has two key components:

1. **Accuracy Penalty:** The first term is simply  $-\text{MSE}(a_{i^*,t}, m_t^*)$ , the negative Mean Squared Error between the winning agent’s score predictions ( $a_{i^*,t}$ ) and the true scores ( $m_t^*$ ). Penalising inaccurate predictions provides a signal for each agent’s actor to provide scores which are true to the state and capabilities of the node it is evaluating, rather than scores which are arbitrarily high, thus encouraging agents to learn a calibrated, meaningful evaluation function.
2. **Success Bonus:**  $B$  is a small, constant bonus given for any successful placement. This positive signal for making a placement ensures the system isn’t too conservative, and that learning is focused on doing useful work.

This scalar reward signal  $R_t$  is then communicated to all the agents. This global feedback is key, as it allows the entire population to learn from the outcome of every individual scheduling event, regardless of which of the competing agents was ultimately chosen as the winner. This allows the entire population to share experiences, and ultimately, leads to the emergence of coordinated, globally optimal scheduling strategies. Finally, we choose a discount factor  $\gamma$  with a value close to 1 (e.g. 0.99). This causes the agents to be far-sighted, i.e. to place strong weight on future rewards during their policy updates. This is key for our problem domain, as we want to incentivise the emergence of policies that lead to long-term system stability and efficiency, as opposed to myopic, short-term gain-seeking behaviours.

## 3.2 System Architecture and Decentralised Execution

The AGMARL-DKS framework is composed of two primary architectural components: a shared Graph Neural Network for contextual state enrichment, and a set of Node Agents, each with an actor-critic architecture [53]. These components work in concert to enable the learning of sophisticated, coordinated scheduling policies.

### 3.2.1 Graph Neural Network for Context-Aware Observations

Implicit coordination is facilitated by passing the global cluster state through a shared GNN at each timestep. We model the cluster as a fully connected graph  $\mathcal{G}_t = (V, E)$  where  $V$  are the cluster’s worker nodes and  $E$  are the edges between these nodes. We assign each node  $i$  its raw feature vector  $h_{i,t}^{(0)}$ .

A multi-layer GNN is applied on graph  $\mathcal{G}_t$  to obtain a context-aware embedding for each node. This is done using a message-passing mechanism, in which each node iteratively aggregates messages from its neighbours and updates its own representation. For layer  $k$  of the GNN, the hidden state (or feature vector)  $h_{i,t}^{(k)}$  for node  $i$  is updated as follows:

$$h_{i,t}^{(k+1)} = \sigma \left( W_1^{(k)} h_{i,t}^{(k)} + W_2^{(k)} \sum_{j \in \mathcal{N}(i)} \frac{h_{j,t}^{(k)}}{|\mathcal{N}(i)|} \right)$$

where:

- $\mathcal{N}(i)$  is the set of neighbouring nodes to node  $i$ .
- $h_{j,t}^{(k)}$  is the feature vector of a neighbouring node  $j$  at layer  $k$ .
- $W_1^{(k)}$  and  $W_2^{(k)}$  are trainable weight matrices for layer  $k$ , shared across all nodes.  $W_1^{(k)}$  transforms the node’s own representation, while  $W_2^{(k)}$  transforms the aggregated information from its neighbours.
- $\sigma$  is a non-linear activation function, such as ReLU.

After  $K$  layers of message passing, the final output of node  $i$  is a dense embedding vector  $e_{i,t} = h_{i,t}^{(K)}$ . Our dense embedding representation encodes complex structure details and dependencies that span multiple hops within the neighbourhood of node  $i$ , which covers the whole cluster because of the fully connected graph structure [52]. This GNN embedding for each node is then concatenated to the respective raw feature vector to form the final local observation for agent  $i$ :

$$o_{i,t} = \text{concat}(h_{i,t}^{(0)}, e_{i,t})$$

This ensures that each agent has a rich, localised perception that is also aware of the global context of the whole system, which is necessary to learn coordinated behaviour without communication.

### 3.2.2 Node Agent Actor-Critic Architecture

The actor-critic model of Agent  $i$  utilizes two neural networks which undergo updates during centralised training [48].

### **Actor Network**

Agent  $i$ 's Actor Network  $\mu_{\theta_i}$  is its policy function. It maps from local observations to actions [53]. It is implemented as a feed-forward neural network parametrised by  $\theta_i$ . At each timestep  $t$ , it takes the agent's GNN-enhanced local observation  $o_{i,t} \in \mathbb{R}^{26}$  as input, and outputs a deterministic action vector  $a_{i,t} \in [0, 1]^3$ . The action vector produced by the agent represents its learned scores across three objectives which are Fault Tolerance, Utilisation and Cost.

The computation through the network's layers can be expressed as:

$$\begin{aligned} h_1 &= \text{ReLU}(W_1 o_{i,t} + b_1) \\ h_2 &= \text{ReLU}(W_2 h_1 + b_2) \\ a_{i,t} &= \mu_{\theta_i}(o_{i,t}) = \sigma(W_3 h_2 + b_3) \end{aligned}$$

where:

- $h_1 \in \mathbb{R}^{128}$  and  $h_2 \in \mathbb{R}^{64}$  are the outputs of the two hidden layers, respectively.
- $W_1 \in \mathbb{R}^{128 \times 26}$ ,  $W_2 \in \mathbb{R}^{64 \times 128}$ , and  $W_3 \in \mathbb{R}^{3 \times 64}$  are the weight matrices.
- $b_1 \in \mathbb{R}^{128}$ ,  $b_2 \in \mathbb{R}^{64}$ , and  $b_3 \in \mathbb{R}^3$  are the bias vectors.
- $\text{ReLU}(\cdot)$  is the Rectified Linear Unit activation function.
- $\sigma(\cdot)$  is the element-wise sigmoid activation function, normalising the final three objective scores to  $[0, 1]$ . This bounded output is important for learning stability as well as the lexicographical selection mechanism that follows.

### **3.2.3 Hybrid Action Selection Mechanism**

The final action selection is based on a hybrid mechanism, which considers the value functions learned by the decentralised agents and a heuristic-based, centralised action selection policy. The hybrid, two-step procedure, which is performed at every scheduling instance, aspires to produce context-sensitive decisions while also maintaining coherence with the overall operational objectives [54].

#### **Step 1: Decentralised Score Generation**

When a new pod scheduling request is received at timestep  $t$ , the environment first prunes the set of all agents to the set of candidate nodes  $\mathcal{C}_t$  based on the hard constraints of the pod (resources, CPU, memory) and Kubernetes rules (taints/tolerations, node affinity).

Each agent  $i$  for which  $i \in \mathcal{C}_t$  runs its actor network  $\mu_{\theta_i}$  with its local GNN-augmented observation  $o_{i,t}$  as input and outputs its action vector  $a_{i,t}$  as the multi-objective score for the requested pod:

$$a_{i,t} = \mu_{\theta_i}(o_{i,t}) = [\text{score}_{\text{FT}}, \text{score}_{\text{UTIL}}, \text{score}_{\text{COST}}]$$

The set of all actions  $\mathbf{a}_t = \{a_{i,t} \mid i \in \mathcal{C}_t\}$  from candidate agents represents the joint decentralised learned evaluation of all candidate nodes over all 3 objectives (Fault Tolerance, Utilisation, and Cost) and is used as input to the centralised selection stage.

### Step 2: Centralised Lexicographical Filtering

The joint action  $\mathbf{a}_t$  is forwarded to the central scheduler extender which runs a deterministic lexicographical filtering algorithm to select the final winning node [55]. The algorithm proceeds in three steps:

1. **Stress-Aware Objective Prioritisation:** The current global system stress level  $L_t$  is used to look up a priority-ordered sequence of objectives  $\mathcal{O}_t = [o_1, o_2, o_3]$ . For example, in the case of high stress ( $L_t > \text{threshold}$ ) the lexicographical order might be set to [Fault Tolerance, Cost, Utilisation] while in normal conditions it might be [Utilisation, Cost, Fault Tolerance]. This renders the policy explicitly state-adaptive to the current conditions of the cluster.
2. **Iterative Candidate Filtering:** The algorithm then iteratively filters the set of candidate nodes  $\mathcal{C}_t$ . It starts with the initial set  $\mathcal{C}_0 = \mathcal{C}_t$  and produces a sequence of smaller and smaller sets of candidates  $\mathcal{C}_0 \supseteq \mathcal{C}_1 \supseteq \mathcal{C}_2 \supseteq \mathcal{C}_3$ . For each objective  $o_k$  in the priority-ordered sequence ( $k = 1, 2, 3$ ), the next set of candidates  $\mathcal{C}_k$  is obtained by taking the subset of nodes from the previous set  $\mathcal{C}_{k-1}$  whose score with respect to the considered objective  $o_k$  is near-optimal:

$$\mathcal{C}_k = \{c \in \mathcal{C}_{k-1} \mid \text{score}_{o_k}(c) \geq (1 - \delta_{\text{lex}}) \cdot \max_{c' \in \mathcal{C}_{k-1}} \text{score}_{o_k}(c')\}$$

where  $\text{score}_{o_k}(c)$  is the learned score for objective  $o_k$  obtained by querying the actor of the agent residing at node  $c$ . The parameter  $\delta_{\text{lex}}$  is a small tolerance value (e.g. 0.05) which allows to retain a set of high-scoring nodes, rather than a single best node, at each stage of the algorithm. This ensures that the algorithm does not get stuck early on with a suboptimal set of candidates.

3. **Deterministic Tie-Breaking:** If the last set  $\mathcal{C}_3$  still contains more than one node after the three filtering stages, then a deterministic tie-breaking rule (such as choosing the node with the lowest index) is applied to produce a single winner [56]. The pod is finally bound to the winning node.

This simple hybrid approach enforces a strong separation of concerns. It offloads the complex, fine-grained state-dependent evaluation of which nodes are preferable, to the learned actor networks. But at the same time, the high-level, high-stakes decision of how to trade off between different objectives, is governed by an explicit, interpretable, and stress-aware policy.

### 3.3 Centralised Training and Decentralised Execution

The AGMARL-DKS agents are trained using the Multi-Agent Deep Deterministic Policy Gradient (MADDPG) algorithm [57] which is based on the Centralised Training with Decentralised Execution (CTDE) paradigm [58]. CTDE was designed specifically for the case of multi-agent reinforcement learning, where the main difficulty is non-stationarity. In multi-agent RL, every agent’s policy changes throughout training, meaning that for each agent the environment is non-stationary (as the behaviour of other agents in the environment is part of the state transition dynamics). In such a setting, it is difficult for typical RL algorithms to converge.

CTDE overcomes this by using a centralised critic for training that has access to the global state and actions of all agents. This critic is able to learn a stable action-value function for the joint policy and then at execution time, the need for the centralised information is removed. At test time, each agent will select its own action based on its local observation through its own actor network. The decoupling between the training and execution of CTDE allows for the learning of coordinated policies offline and decentralised and reactive execution online at scale. In addition to CTDE, we use two more methods to increase training stability and data efficiency, these are a shared experience replay buffer and soft updates for target networks.

### 3.3.1 Centralised Critic for Stable Value Estimation

#### *Critic Network*

The Critic Network,  $Q_{\phi_i}$ , is used to approximate the agent’s action-value function. The primary task of the critic network is to learn the centralised training signal, by estimating the expected long-term return (Q-value) for a particular global state and joint action [49, 50]. As with the MADDPG baseline, the critic of agent  $i$  has access to the observations and actions of all the agents in the system, rather than only to the local information available to agent  $i$ . This is necessary for stable multi-agent learning.

In order to scale up to an arbitrary number of agents without a change in architecture, the critic network has the form shown in Algorithm 1, taking as input agent  $i$ ’s local observation  $o_{i,t}$ , agent  $i$ ’s action  $a_{i,t}$ , and the aggregation of the other agents’ observations and actions,  $\{o_{j,t}, a_{j,t}\}_{j \neq i}$ .

The network’s forward pass is structured as follows:

1. **Parallel Processing of Other Agents’ Information:** The observation-action pairs from all other agents ( $j \neq i$ ) are first processed. Each pair is concatenated and passed through a shared feed-forward network, parametrised by  $\phi_{other}$ , to generate an intermediate embedding:

$$z_j = f_{\phi_{other}}(\text{concat}(o_{j,t}, a_{j,t})) \quad \forall j \neq i$$

2. **Aggregation:** These individual embeddings are then aggregated into a single fixed-size vector using mean-pooling [51]. This step ensures the input size to the subsequent layers is independent of the number of agents,  $N$ :

$$\bar{z}_{others} = \frac{1}{N-1} \sum_{j \neq i} z_j$$

In our implementation, this results in a 128-dimensional vector.

3. **Final Q-Value Estimation:** This aggregated vector is concatenated with agent  $i$ ’s own observation and action. The resulting combined vector is then passed through the final layers of the critic network, parametrised by  $\phi_{main}$ , to output a single scalar Q-value:

$$Q_{\phi_i}(o_{i,t}, a_{i,t}, \{o_{j,t}, a_{j,t}\}_{j \neq i}) = f_{\phi_{main}}(\text{concat}(o_{i,t}, a_{i,t}, \bar{z}_{others}))$$

The complete critic function can be formally written as  $Q_{\phi_i}(o_{i,t}, a_{i,t}, \text{agg}(\{o_{j,t}, a_{j,t}\}_{j \neq i}))$ . By learning a function that explicitly considers the actions of all agents, the centralised critic provides a stable learning target for each agent’s actor. This mechanism is the key to overcoming the environmental non-stationarity inherent in multi-agent learning, enabling the agents to develop complex and cooperative strategies.

### 3.3.2 Actor and Critic Updates using MADDPG

#### *Critic Update*

The critic for each agent  $i$ ,  $Q_{\phi_i}$ , is trained to learn the joint action-value function by minimising a loss derived from the Bellman equation [59]. For each transition tuple  $(s, \mathbf{a}, r, s')$  randomly sampled from the shared replay buffer  $\mathcal{D}$ , where  $s$  is the global state,  $\mathbf{a} = \{a_1, \dots, a_N\}$  is the joint action,  $r$  is the global reward, and  $s'$  is the next state. Also, the critic’s parameters  $\phi_i$  are updated by minimising the Mean Squared Error (MSE) loss,  $L(\phi_i)$ :

$$L(\phi_i) = \mathbb{E}_{(s, \mathbf{a}, r, s') \sim \mathcal{D}} \left[ (Q_{\phi_i}(s, a_1, \dots, a_N) - y_i)^2 \right]$$

where  $y_i$  is the one-step temporal difference (TD) target. This target value is computed using the target critic ( $Q'_{\phi_i}$ ) and target actor ( $\mu'_{\theta_j}$ ) networks, which are separate, slowly updated copies of the online networks:

$$y_i = r_i + \gamma Q'_{\phi_i}(s', \mu'_{\theta_1}(o'_1), \dots, \mu'_{\theta_N}(o'_N))$$

Here,  $\gamma$  is the discount factor. The use of target networks is critical for stability; it provides a consistent and slowly moving target  $y_i$ , preventing the oscillations that would occur if the critic were trying to learn from its own rapidly changing value estimates [49]. The centralised nature of the critic is essential, as it conditions on the joint action, allowing it to form a comprehensive and stable learning signal for each agent.

#### *Actor Update*

The actor for each agent  $i$ ,  $\mu_{\theta_i}$ , learns a deterministic policy that maps its local observation  $o_i$  to a specific action  $a_i$ . The actor’s parameters  $\theta_i$  are updated using the deterministic policy gradient theorem [60]. The goal is to adjust the policy in a direction that leads to actions the centralised critic deems more valuable. The actor ascends the gradient of its expected return objective function,  $J(\theta_i)$ , which is given by:

$$\nabla_{\theta_i} J(\theta_i) = \mathbb{E}_{s, \mathbf{a} \sim \mathcal{D}} \left[ \nabla_{\theta_i} \mu_{\theta_i}(o_i) \nabla_{a_i} Q_{\phi_i}(s, a_1, \dots, a_N) \Big|_{a_i = \mu_{\theta_i}(o_i)} \right]$$

This update rule is an application of the chain rule. The term  $\nabla_{a_i} Q_{\phi_i}(\cdot)$  is the gradient from the critic, indicating how agent  $i$ ’s action should change to increase the expected return. This signal is then backpropagated through the actor network via the term  $\nabla_{\theta_i} \mu_{\theta_i}(o_i)$  to update the actor’s parameters. In essence, the actor learns to produce

actions that maximise the long-term, system-wide reward as estimated by the globally-informed centralised critic [48].

### 3.3.3 Training Stability Mechanisms

To ensure the convergence and stability of the learning process, two standard mechanisms are employed.

1. **Experience Replay:** There is a centralised experience replay buffer  $\mathcal{D}$  that contains a large history of past transition tuples. The batch of experiences for each training iteration is sampled uniformly at random from this replay buffer. This technique decorrelates the updates and ensures that the samples obey the i.i.d. assumption needed by stochastic gradient descent, hence stabilising learning [61].
2. **Soft Target Updates:** Each online actor ( $\mu_{\theta_i}$ ) and critic ( $Q_{\phi_i}$ ) network has a corresponding target network ( $\mu'_{\theta_i}$  and  $Q'_{\phi_i}$ ) that is also used to estimate the target value function. The weights of the target networks are not trained through backpropagation, but are updated by slowly tracking the weights of the online networks via Polyak averaging [62]. This update rate  $\tau \ll 1$  is:

$$\theta'_i \leftarrow \tau\theta_i + (1 - \tau)\theta'_i \quad \text{and} \quad \phi'_i \leftarrow \tau\phi_i + (1 - \tau)\phi'_i$$

This "soft" update, in contrast to a hard reset or a direct copy, ensures that the TD target  $y_i$  changes slowly and in a predictable way which is helpful to avoid policy divergence and stabilize training.

---

**Algorithm 1** AGMARL-DKS Training Process (MADDPG with Hybrid Policy)

---

```
1: Initialize:
2: for all agent  $i = 1, \dots, N$  do
3:   Actor network  $\mu_{\theta_i}$  and Critic network  $Q_{\phi_i}$  with random weights.
4:   Target networks  $\mu'_{\theta_i} \leftarrow \mu_{\theta_i}$  and  $Q'_{\phi_i} \leftarrow Q_{\phi_i}$ .
5: end for
6: Shared GNN  $\mathcal{G}_{\text{nn}}(\theta^{\text{GNN}})$ .
7: Shared Replay Buffer  $\mathcal{D}$ .
8: for episode  $e = 1, \dots, E_{\text{max}}$  do
9:   Get initial global state  $s_t$  and stress level  $L_t$ .
10:  for step  $t = 1, \dots, T_{\text{max}}$  do
11:    // Decentralized Score Generation
12:    Use GNN to compute embeddings  $e_t$  from  $s_t$ .
13:    Form local observations  $o_{i,t}$  for each agent  $i$ .
14:    Get joint action (all scores)  $\mathbf{a}_t = \{\mu_{\theta_1}(o_{1,t}), \dots, \mu_{\theta_N}(o_{N,t})\}$ .
15:    // Centralized Winner Selection
16:    Identify candidate nodes  $\mathcal{C}_t$  based on pod requirements.
17:    Select winning agent  $i^* \leftarrow \text{LexSelect}(\{a_{i,t} \mid i \in \mathcal{C}_t\}, L_t)$ .
18:    // Environment Interaction
19:    Execute placement on node  $i^*$ , observe outcome.
20:    Compute shared reward  $R_t$  and get next global state  $s_{t+1}$ .
21:    Store transition tuple  $(s_t, \mathbf{a}_t, R_t, s_{t+1})$  in  $\mathcal{D}$ .
22:     $s_t \leftarrow s_{t+1}$ .
23:    // Centralized Training Step
24:    if  $|\mathcal{D}| < \text{BATCH\_SIZE}$  then continue
25:    end if
26:    Sample a random minibatch of transitions from  $\mathcal{D}$ .
27:    for all agent  $i = 1, \dots, N$  do
28:      // Update Critic  $Q_{\phi_i}$ 
29:      Set target  $y_i = r_i + \gamma Q'_{\phi_i}(s', \mu'_{\theta_1}(o'_1), \dots, \mu'_{\theta_N}(o'_N))$ .
30:      Update critic by minimizing loss:  $L(\phi_i) = (Q_{\phi_i}(s, \mathbf{a}) - y_i)^2$ .
31:      // Update Actor  $\mu_{\theta_i}$ 
32:      Update actor using the policy gradient:  $\nabla_{\theta_i} J \approx \nabla_{a_i} Q_{\phi_i}(s, \mathbf{a})|_{a_i=\mu_i(o_i)} \nabla_{\theta_i} \mu_{\theta_i}(o_i)$ .
33:    end for
34:    // Soft Target Network Updates
35:    Update all target networks:  $\theta'_i \leftarrow \tau \theta_i + (1 - \tau) \theta'_i$ ,  $\phi'_i \leftarrow \tau \phi_i + (1 - \tau) \phi'_i$ .
36:  end for
37: end for
```

---

## 4 System Design

The proposed system, illustrated in Fig 2, offers an advanced pod placement solution for Kubernetes that uses a multi-objective approach to achieve efficient fault tolerance in parallel with resource utilisation and operational cost management. The architecture diagram demonstrates how a development pipeline for scheduling models merges with a Kubernetes deployment environment to both execute and test runtime behaviour.

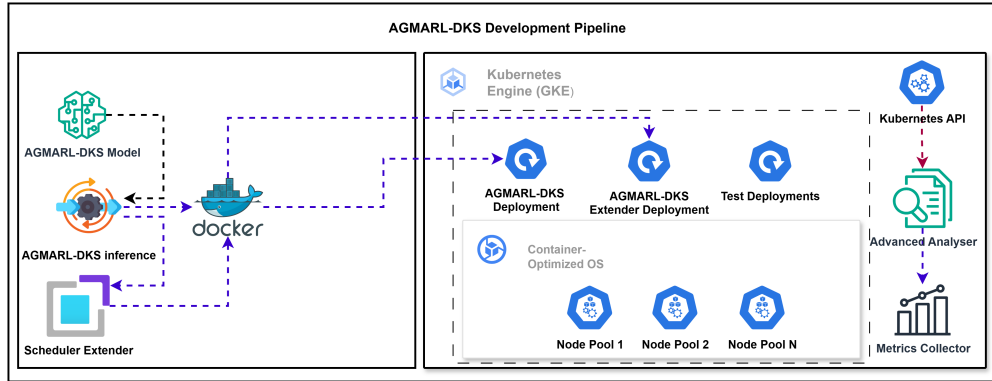


**Fig. 2:** The high-level architecture design for the AGMARL-DKS implementation in GKE

## 4.1 Development Pipeline

The Development Pipeline begins with the AGMARL-DKS Model training process. A sophisticated training phase occurs within a high-fidelity simulated Kubernetes environment. This environment is designed to bridge the sim-to-real gap by generating nodes that demonstrate realistic characteristics derived directly from the Kubernetes API, such as node `conditions` (e.g., `MemoryPressure`), `taints`, and `labels`. This replaces a prior dependency on abstract metrics.

The actor and critic models for each agent are trained to assess state-action pairs by using an enhanced state representation that is consistent between the simulation and a live cluster. The state vector includes normalised resource availability (CPU, RAM), binary flags for node conditions, a count of node taints, and Graph Neural Network (GNN) embeddings, all contextualised by a global cluster stress factor. The training process uses a reward function that combines fault tolerance, resource utilisation, and cost metrics into a weighted composite which changes according to the simulated cluster stress levels, as detailed in Section 3.4. The training process employs lexicographical action selection during exploration to balance between various objectives and saves the trained critic and GNN model weights upon completion.

The AGMARL-DKS Inference module loads these pre-trained model weights after training. This inference agent is designed to load the pre-trained actor model for each node agent and is designed to compute a multi-objective score vector for each candidate node by constructing the same augmented state vector from live cluster data and executing the critic model.

The Scheduler Extender then integrates this inference function with the Kubernetes scheduling process. It is implemented as a Flask web application with filtering and prioritising HTTP endpoints, which are called by the main Kubernetes scheduler. When a request is received, the extender retrieves the current, real-world state of the nodes (resource availability from the Metrics API, node conditions, and taints), predicts the total cluster stress, and scores every node by using the AGMARL-DKS

Inference Agent. The entire Scheduler Extender, including the inference logic and model weights, is packaged into a Docker container image for deployment.

## 4.2 Kubernetes Deployment Environment

The operational components of the AGMARL-DKS system operate within a standard Google Kubernetes Engine (GKE) [64]. The AGMARL-DKS *Scheduler Deployment* creates a `kube-scheduler` instance that is configured via a ConfigMap to use an external HTTP extender for the filtering and prioritisation phases of the scheduling cycle.

The AGMARL-DKS *Scheduler Extender Deployment* contains the actual intelligent decision-making logic. This deployment runs the Docker container housing the Flask application and the trained inference models. The aim is to receive the multi-objective score vectors from the inference agent and apply the lexicographical filtering logic to determine the final node priorities. A Kubernetes service exposes the extender’s endpoints internally, allowing the main scheduler to communicate with it. The *node pool* consists of virtual machines that host the user workloads (pods). All system components interact through the central *Kubernetes API*. Finally, *Test Deployments* are used to deploy workloads specifically assigned to either the default scheduler or the AGMARL-DKS scheduler, enabling direct performance comparisons.

## 4.3 Monitoring and Analysis

The system uses an *Advanced Analyser* and a *Metrics Collector* for its monitoring and analysis functions. The Advanced Analyser is a Python script which delivers comprehensive cluster health assessments by checking container statuses for problems such as `CrashLoopBackOff` or `OOMKilled`, evaluating Deployment health, examining node conditions like `MemoryPressure`, and reporting critical Kubernetes events. The Metrics Collector uses both the Kubernetes API and the Metrics Server to gather extensive time-series data, covering pod resource usage, requests, restart counts, and scheduler assignments, alongside node capacity and utilisation data. The script combines and aggregates data from multiple test runs to produce a series of comparative plots. These visualizations demonstrate how the different schedulers perform across key metrics, including pod distribution patterns, resource utilisation, pod failure rates, and stress-level adaptation.

## 5 Experimental Setup

This section presents the experimental methodology used to evaluate the AGMARL-DKS scheduling agent in comparison to the baseline Kubernetes default scheduler. The Google GKE environment served as the setting for our evaluation, which examined the cluster infrastructure, scheduler configurations, the robust synthetic workload design, and the metrics collection mechanisms.

## 5.1 Experimental Setup and Cluster Infrastructure

To evaluate our approach, we ran experiments on Google Kubernetes Engine (GKE). We configured GKE to be as realistic, highly available, and heterogeneous as possible for a production environment. A regional cluster was created for high availability in a specific region. Additionally, to avoid additional experiment artefacts, we configured the GKE cluster with VPC-native networking and specified dedicated subnets and secondary IP ranges for Pods and Services. This setup avoids Pod and Service IP address exhaustion during large-scale and high-churn experiments.

The cluster consisted of two separate node pools, in an attempt to create a heterogeneous environment that could handle both general and more demanding workloads. The configuration details for the pools can be seen below in Table 2.

**Table 2:** GKE Node Pool Configurations for Experimental Scenarios

Node Pool Name	Machine Type	vCPUs	Memory (GB)	Node Count
baseline-pool	e2-standard-4	4	16	3 (Fixed)
stress-pool	e2-highmem-4	4	32	1-5 (Autoscaled)

This configuration provided a dynamic total cluster capacity ranging from a baseline of 4 nodes (16 vCPUs, 80 GB memory) to a maximum of 8 nodes (32 vCPUs, 208 GB memory). All nodes operated on Google’s Container-Optimised OS with the containerd container runtime.

The experimental setup incorporates both fixed and autoscaled node pools to achieve balanced performance assessment. We maintained the `baseline-pool` at a constant size of three nodes, which provided a stable and static reference point for evaluating schedulers under uniform conditions. On the other hand, autoscaling is explicitly enabled for the `stress-pool`, as this is of key importance for fault-injection and high-churn scenarios (Scenario 2), where the focus lies on the scheduler’s performance, not on a constant topology, but rather in a dynamically adapting cluster size with changing amounts of available resources as a result of stress-induced churn.

## 5.2 Workload Design and Deployment

For a more quantitative and empirical evaluation of AGMARL-DKS, a set of intensive experiments was conducted to analyse the behaviour of schedulers in a dynamic, heterogeneous, and adversarial setting, moving beyond conventional, fixed benchmarks. As such, we introduce a two-pronged evaluation framework that consists of two distinct stress tests. The goal of each stress test is to create a unique and adversarial set of system-wide pressures that challenge specific aspects of a scheduler’s intelligence. The section describes two specific tests which include the *Cascading Resource Pressure Test* and the *Volatile Churn and Fault Injection Test*. We applied uniform workloads to both the Kubernetes default scheduler and the AGMARL-DKS agent, enabling a straightforward comparative analysis.

**Table 3:** Experimental protocol for Scenario 1: cascading resource pressure test

Ph.	Time	Workload	Profile	Stress	Goal
I	0–10	100 <code>nginx</code> Pods	Static, minimal requests (100 mCPU, 128 MiB). Stable and long-lived.	Low	Baseline performance and initial pod distribution.
II	10–20	75 <code>stress-ng</code> Pods	250 mCPU, 512 MiB. Latent memory spike to 1 GiB after 5 min.	Medium	Response to dynamic workload and emerging node pressure.
III	20–30	150 <code>nginx</code> Pods	Heterogeneous, high-demand (avg. 500 mCPU, 800 MiB).	High	Bin-packing and load balancing under peak load.
IV	30–40	20 Batch Jobs	Very large, non-preemptive (1.5 CPU, 2 GiB). Designed to oversaturate.	Extreme	Scheduler behaviour under severe scarcity and contention.

**Table 4:** Experimental protocol for Scenario 2: volatile churn and fault injection test

Ph.	Time	Workload	Profile	Stress	Goal
I	0–30	150 <code>busybox</code> + 120 <code>stress-ng</code> Pods	Liveness probes fail after 60 s; forced restarts. Pods end with <code>OOMKilled</code> .	High	Maintain stability and avoid problematic nodes under constant pod churn.
II	15–30	50 Batch Jobs	Short-lived (90 s) with high, bursty resource requests (1 vCPU, 1 GiB).	Extreme	Evaluate scheduling latency and efficiency for high-priority tasks amid background chaos.
III	30–45	Node failure simulation	<code>NoSchedule</code> taint applied to a highly-utilized worker node, removing it from the schedulable pool.	Extreme	Assess adaptive rescheduling and redistribution of workloads under infrastructure failure.

### 5.2.1 Scenario 1: Cascading Resource Pressure Test

This scenario evaluates each scheduler’s ability to optimise resource packing and load balancing while assessing its performance in preventing total system starvation under maximum or near-maximum resource usage levels. To achieve this, as shown in Table 3, we first increase the cluster’s utilization slowly, then rapidly, and then to maximum to create as much stress on the cluster as possible, to understand more about how each scheduler performs resource packing and load balancing as well as how it can avoid a node starving state like `MemoryPressure`.

### 5.2.2 Scenario 2: Volatile Churn and Fault Injection Test

This scenario is engineered to evaluate each scheduler’s resilience and fault-tolerant capabilities, which are central claims of the AGMARL-DKS framework. The objective is to quantify the ability to maintain system stability and service availability in a chaotic environment where the primary stress vector is not resource exhaustion, but rather high-frequency control plane operations and unpredictable infrastructure failures. The experimental protocol, outlined in Table 4, creates a sustained high-churn environment through workloads specifically designed to exhibit common failure modes. This scenario directly tests the efficacy of the fault-tolerance objective prioritised by

the AGMARL-DKS agent. The introduction of a simulated node failure via ‘NoSchedule’ tainting provides a critical test of the scheduler’s ability to adapt dynamically to sudden, drastic reductions in available cluster capacity.

The combination of these two scenarios provides a comprehensive and multi-faceted evaluation of scheduler performance. Scenario 1 rigorously tests the economic and efficiency aspects of resource allocation, while Scenario 2 directly validates the critical, non-functional requirements of resilience and fault tolerance that are essential for production-grade systems.

## 6 Experimental Results and Analysis

This section presents a comprehensive empirical analysis of the AGMARL-DKS scheduler’s performance in comparison to the standard Kubernetes default scheduler, focusing on the results from the *Cascading Resource Pressure Test* (Scenario 1) as detailed in Section 5.2. The analysis herein examines performance related to resource management, intelligent workload distribution, and adaptive load balancing under conditions of progressively increasing systemic stress. The results pertaining to fault tolerance from Scenario 2 will be presented subsequently.

### 6.1 Scenario 1: Performance under Cascading Resource Pressure

This test tries to show how each scheduler behaves in its core resource management role as the load on the system gradually increases. This can be seen on two axes: the general strategy for distributing the workload, and how this strategy is adjusted as more load and pressure on the available resources is put on the system. Note that in the Default scheduler graphs, the mad4pg-scheduler and mad4pg-scheduler-extender pods are visible as well. That is not a mistake; since our custom scheduler is not started until after the kube-scheduler has finished its pass over the system, by default, the kube-scheduler does the first placement of everything, including our scheduler’s own pods. The scheduler’s pods do not consume many resources, so their presence should not affect the relative performance.

#### 6.1.1 Workload Distribution and Resource Consolidation

The placement of the overall workload clearly shows the distinct philosophies of the two schedulers. Figure 3 shows a heatmap of the number of pods in each application type and on each node, demonstrating the Default scheduler’s load-balancing strategy. The Default scheduler places pods from every type of application onto as many nodes as possible. This is more true for the nginx-baseline and peak-demand workloads, as can be seen. The Default scheduler has load balancing as a primary goal, so it spreads pods around to prevent overloading any one node. In contrast, the AGMARL-DKS agent is enforcing a learned, smart packing strategy. This agent is much more inclined to concentrate certain workloads onto a small number of nodes. The nginx-baseline pods are densely installed across only 3 nodes according to the given setup. The agent’s policy has likely learned that this is an optimal decision for this workload based on

this type of resource profile (CPU, Memory, other features), or other factors that it has learned from the environment. This is an intentional policy that has been learned to try to optimise resource utilisation as opposed to simply balancing it.

The rationale behind this behaviour is more easily understood by looking at the total requested CPU utilisation per node, as shown in Figure 4. As expected, the flat, homogeneous profile for the Default scheduler is largely caused by utilisation. In contrast, AGMARL-DKS creates a heterogeneous profile in which a number of nodes are more densely packed to very high utilisation. This is not a side-effect of a lack of load balancing; instead, it is a direct consequence of performing it smartly by packing together. This allows AGMARL-DKS to use more effectively the capacity of those nodes, while leaving latent capacity available on other nodes. The system remains responsive while ensuring available resources for scheduling high-priority or bursty future deployments which helps avoid resource fragmentation.

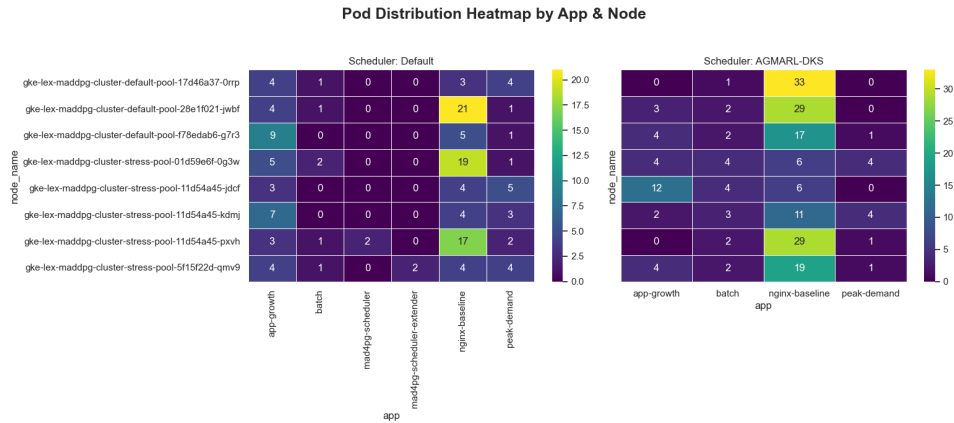


**Fig. 3:** Pod distribution heatmap at the conclusion of Scenario 1. The default scheduler (left) exhibits a scattered placement. The AGMARL-DKS scheduler (right) demonstrates a consolidation strategy, grouping specific application types onto preferred nodes.

This observation is further substantiated by an analysis of the requested CPU utilisation on each node, as shown in Figure 4. The default scheduler achieves a superficially balanced load, with most nodes carrying a similar total CPU request. The AGMARL-DKS scheduler, however, produces a more varied utilisation profile. This is not a sign of poor balancing, but rather an emergent property of its intelligent packing strategy. By concentrating certain workloads, it more effectively utilizes the capacity of those nodes while intentionally leaving other nodes with greater available capacity, potentially preserving them for future high-priority or bursty workloads.

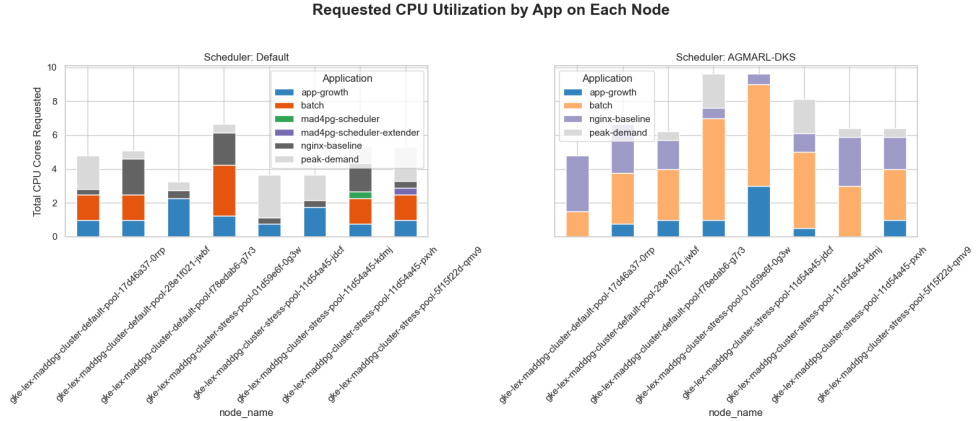


**Fig. 4:** Total requested CPU cores on each node, stacked by application type. The default scheduler (left) creates a relatively even but undifferentiated load. The AGMARL-DKS scheduler (right) creates a more varied load profile, indicating a specialized packing strategy.

### 6.1.2 Adaptive Placement and High-Density Packing under Extreme Stress

The AGMARL-DKS framework posits that its trained agents develop dynamic policy adaptations to manage stresses impacting global system states. Evidence for this is seen in the results of Scenario 1 across phases. In both low and medium utilization (Figures 6 and 7) the AGMARL-DKS agent shows its consolidation approach in the results from low and medium stress scenarios and by exhibiting strong node preferences for `nginx-baseline` and `app-growth` pods, respectively. The effects of this learned intelligence are most demonstrably seen in the high and extreme cases. In the high stress phase (Figure 8), the AGMARL-DKS agent deploys the peak demand workload onto a distinct set of nodes than those used during the medium stress phase, and thereby shows that it has learned an affinity between a given workload and which nodes it prefers.

The most evident contrast emerges when stress reaches its peak as schedulers must position highly demanding batch jobs within the system (Figure 9). The Default scheduler, unwavering in its spread-the-load policy, deploys the batch jobs across nodes with a very low and evenly distributed CPU request across all of them. This is the worst-case policy for high-performance computing workloads like these as it does not use the full capacity of any given node and also leaves resources of those nodes unallocated and unreserved. In contrast, the AGMARL-DKS agent shows a very aggressive packing behaviour. It smartly chooses the right nodes and it requests the highest CPU cores for these kinds of workloads. Indeed, the results prove AGMARL-DKS' capabilities in dealing with mission-critical workloads. This behavior is demonstrably a very complicated, learned policy: by aggressively packing these very compute intensive, non-latency sensitive batch workloads, the agent is achieving the highest throughput

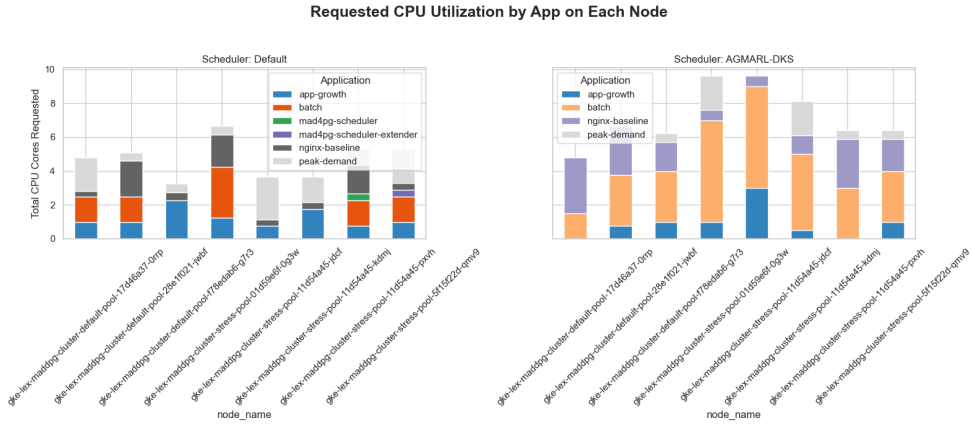


Fig. 5: Stacked CPU utilization.

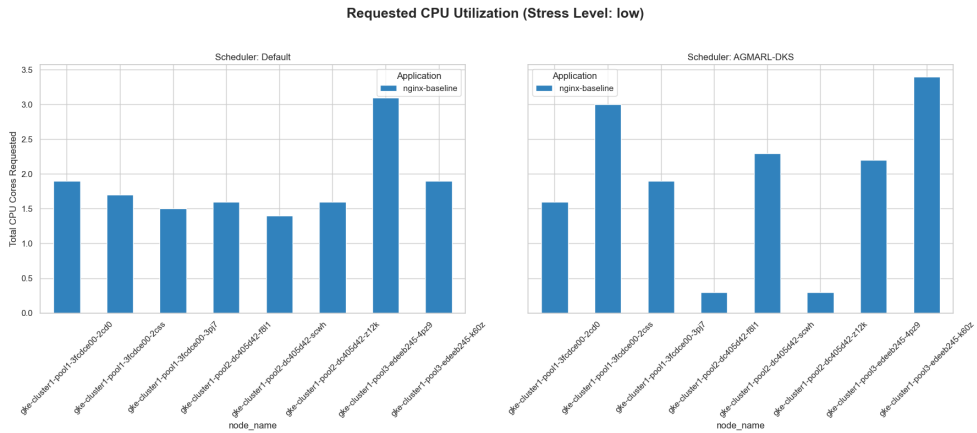


Fig. 6: Requested CPU utilization under low stress.

possible in their execution by dedicating nodes to the task and also simultaneously localizing the risk associated with large resource consumption while also maintaining the other available nodes in a state of low utilization to free them for potentially more important or latency sensitive workloads that may arrive. This also shows that the AGMARL-DKS agent has learned a non-linear, stateful policy that is aware of the lexicographically ordered objectives it was provided, and in this case, has learned to apply very high-density packing when under maximal duress to achieve better efficiency and throughput in the system.

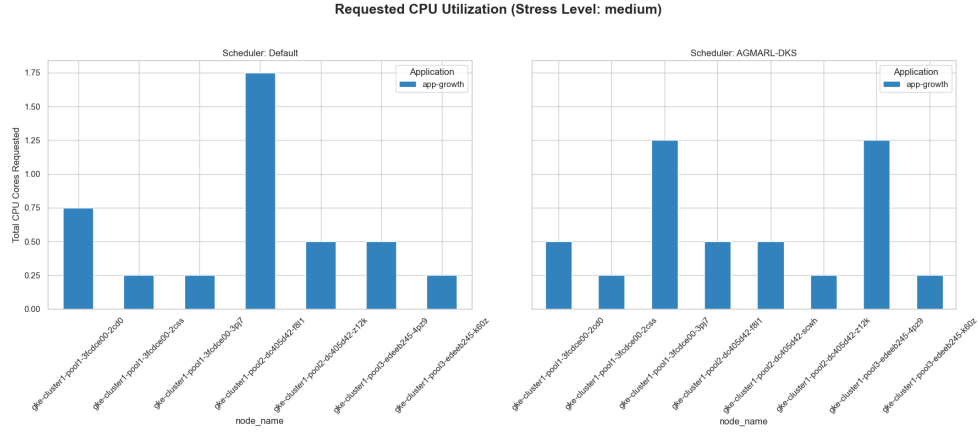


Fig. 7: Requested CPU utilization under medium stress.

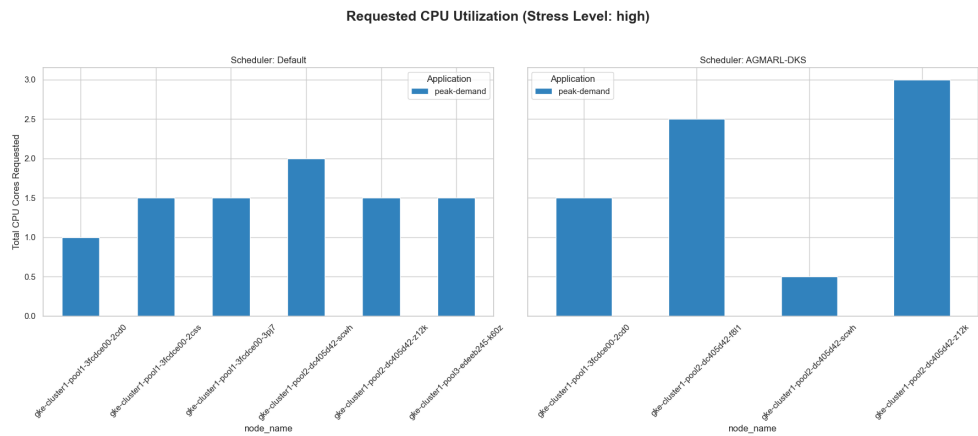


Fig. 8: Requested CPU utilization under high stress.

## 6.2 Scenario 2: Performance under Volatile Churn and Fault Injection

This test scenario was designed to test the resilience and fault tolerance capabilities of each scheduler according to the AGMARL-DKS framework’s main properties. The cluster underwent stress testing in a turbulent environment characterised by high pod churn while applications were randomly terminated during the last phase of processing high-priority bursty workloads.

### 6.2.1 Intelligent Capacity Management and Strategic Self-Restraint

A sophisticated scheduler excels by managing increased throughput without overwhelming the system, sometimes through deliberate pod placement limitations.

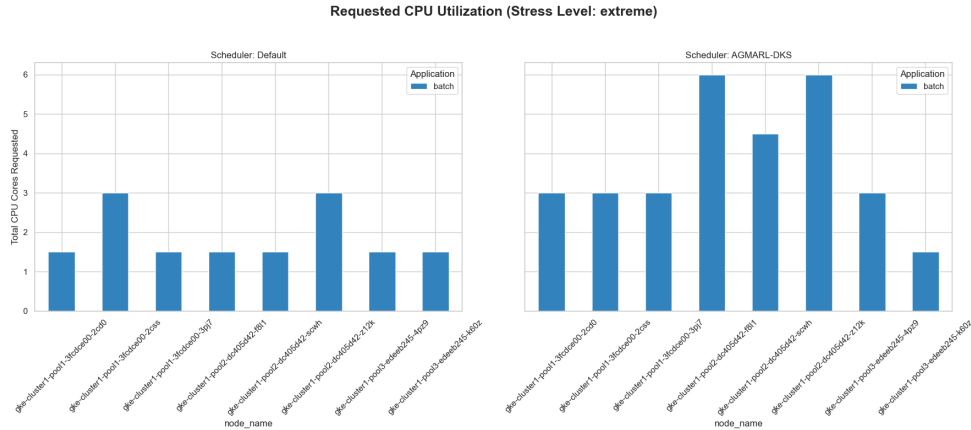
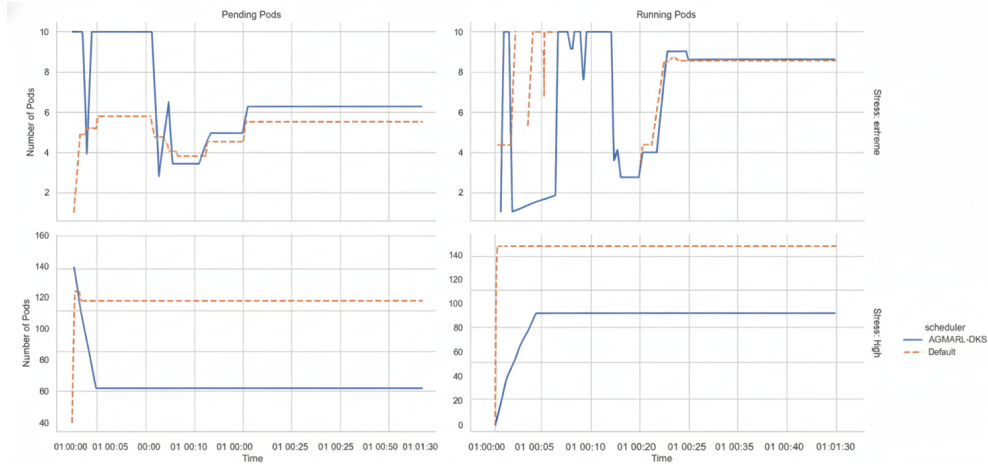


Fig. 9: Requested CPU utilization under extreme stress.

Figure 10 shows one such example of this behaviour, which can be seen clearly during the high-stress phase. As expected, the Default scheduler (being duty-bound to schedule everything it can as quickly as possible) immediately attempts to schedule all 150 liveness-fail pods. However, in a learned and planned action, the AGMARL-DKS agent chooses to only schedule around 100 pods at this point, choosing to leave the remaining pods in pending state. The agent demonstrates controlled action by choosing not to schedule all pods, despite having the capacity to do so. The agent, through its GNN-augmented observation, is aware that the state of the cluster is (becoming) unhealthy from the high churn. Its learned policy thus rightly decides that scheduling the entire workload would violate its hard constraint of staying in a fault-tolerant region and lead to cascading failures. By scheduling less of the unstable pods, it leaves headroom of cluster capacity and stability. The effectiveness of this technique becomes apparent when the system faces subsequent high stress phases. The AGMARL-DKS scheduler maintains system stability while high-priority burst jobs enter the queue and manages to clear its pending jobs in less than sixty seconds. The Default scheduler continues to manage the system instability from its earlier actions, which leads to unpredictable and slow scheduling of the high-priority tasks.

### 6.2.2 Fault-Tolerant Placement and Mitigation of Failure Hotspots

The key analysis point of this stress test involves how well schedulers can control and reduce the detrimental effects generated by faulty workloads. The restart heatmap of the liveness-fail application (Figure 11a) provides a clear indication of the difference in risk propagation. The Default scheduler places pods in a way that produces extreme concentrations of failure: four out of the five nodes see more than 325 restarts each. In other words, the Default scheduler fails to notice the problematic behaviour on those nodes, or at least to take appropriate action to contain that behaviour. The AGMARL-DKS scheduler exhibits risk awareness capabilities that are orders of magnitude more powerful compared to other schedulers. To be sure, it cannot prevent restarts from



**Fig. 10:** Number of Pending and Running pods over time during Scenario 2. Under high stress, AGMARL-DKS (solid line) schedules fewer unstable pods than the default scheduler (dashed line), allowing it to service extreme stress burst jobs more effectively.

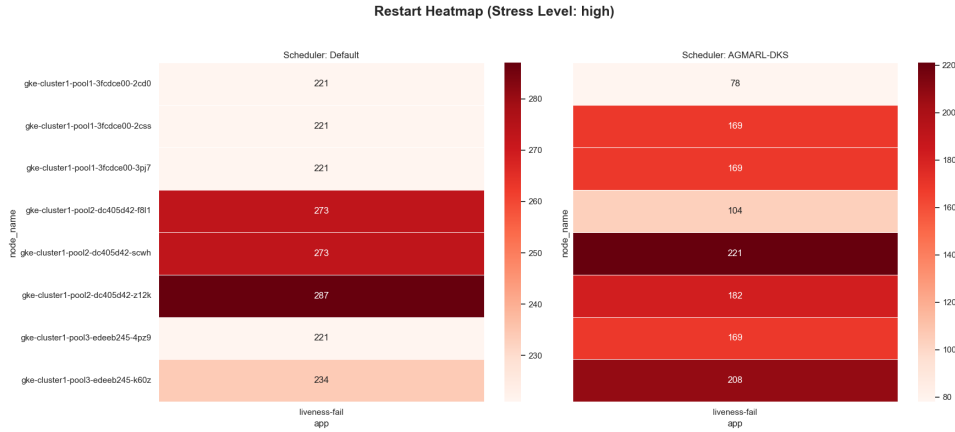
happening in the first place, given the application’s liveness-failure behaviour. But it certainly can prevent the creation of such extreme concentrations of failure. There is still one node (...-28e1f021-jwbf) where the pod placement logic correctly places the majority of the oom-fail pods due to the node’s high stability, but that node is effectively quarantined, and the remaining faulty pods are more evenly distributed, with one node having as few as 130 restarts. The agent has clearly learned to avoid actively overloading nodes that are already manifesting strong indications of instability.

The effectiveness of this risk-aware placement logic is corroborated in the pod distribution heatmap in a state of high stress (Figure 11b). The AGMARL-DKS agent protected node (...-17d46a37-0rrp) stability for non-risk workloads by preventing the placement of memory-intensive oom-fail pods. Through its lack of risk awareness, the Default scheduler indiscriminately positions both faulty workload types throughout the cluster and causes system-wide instability.

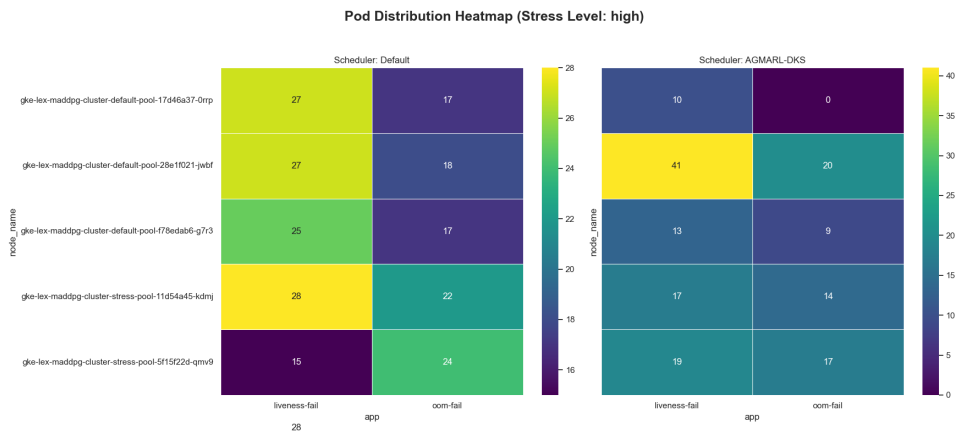
### 6.2.3 Decoupling of Performance Objectives

AGMARL-DKS long-term achievement depends on its ability to learn how to handle complex non-linear trade-offs among various performance targets. Figure 12 shows the Pearson correlation matrix for key performance metrics, which reveals deep insight into the learned policies. The Default scheduler exhibits a strong positive 0.72 correlation between  $mem\_requested\_gb$  and failures as well as restarts. The data reveals the intrinsic negative relationship between system stability and resource demands because increased memory requests lead to higher failure rates.

In contrast, AGMARL-DKS achieves a strong decoupling of these objectives. Its correlation between  $mem\_requested\_gb$  and failures or restarts is exactly -1.00. This



(a) Restart heatmap for ‘liveness-fail’ pods.



(b) Distribution of faulty ‘oom-fail’ pods.

**Fig. 11:** Analysis of fault-tolerant placement under high stress. Subfigure (a) shows that the AGMARL-DKS scheduler mitigates restart hotspots. Subfigure (b) shows it isolates high-risk ‘oom-fail’ pods to a subset of nodes, unlike the default scheduler, which distributes them widely.

remarkable result does not mean that requesting more memory causes fewer failures. Rather, this means that the agent has learned a policy where its fault-tolerance decisions are made completely independently of the pods’ resource requests. The properties of a given pod that affect its stability score (which, we hypothesise, includes node health, historical restart rate, and other complex metrics from the GNN) are orthogonal to those that affect its resource utilisation score. This ability to make informed, risk-aware decisions that are not dominated by simple resource utilisation

metrics is the core value of the AGMARL-DKS framework, and this is unambiguously demonstrated by these results.

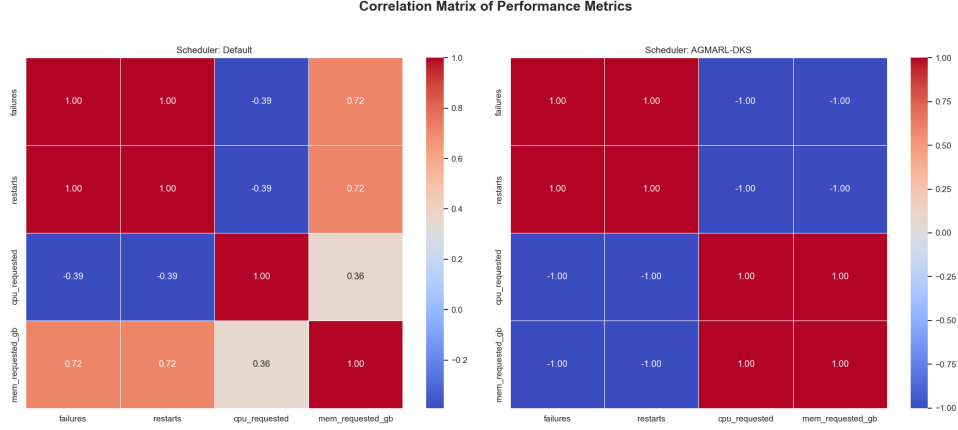


**Fig. 12:** Correlation matrix of performance metrics. The default scheduler (left) shows a strong link between memory requests and failures. The AGMARL-DKS scheduler (right) successfully decouples these objectives, indicating a more sophisticated, fault-aware scheduling policy.

### 6.3 Holistic Performance and Multi-Objective Trade-offs

A key performance indicator of a scheduler is its ability to reach a better-balanced point in the multi-dimensional solution space. An effective scheduler can always find a better assignment for any request by striking an improved balance between fault tolerance and resource usage while managing cost. This is evaluated in the pairplots in Figure 13 and Figure 14, which plots the metrics for the two schedulers, in both test cases.

Under the resource-constrained Scenario 1 (Figure 13), which corresponds to the high performance at increasing resource pressure, AGMARL-DKS scheduler (orange) presents an obviously better and more consistent policy. As can be seen in the distribution plots on the diagonal of the figure, the outcomes of AGMARL-DKS agent have not only a lower mean on the metric (cost, failures, restarts) than the Default scheduler (blue), but also a much smaller variance. In addition, from the scatter plots, we can see that its solutions are more concentrated in the favourable low-cost and low-failure region, demonstrating that its smart packing strategy can effectively improve the resource utilisation without being penalised by the cost and stability. On the other hand, those of Default are more scattered with an apparent tail on the failure distribution, suggesting the agent’s tendency to enter unpredictable and high-failure states when the cluster is stressed.

The performance gap becomes more pronounced during the chaotic failure conditions of Scenario 2 (Figure 14). In this figure, the scattered outcomes from Default

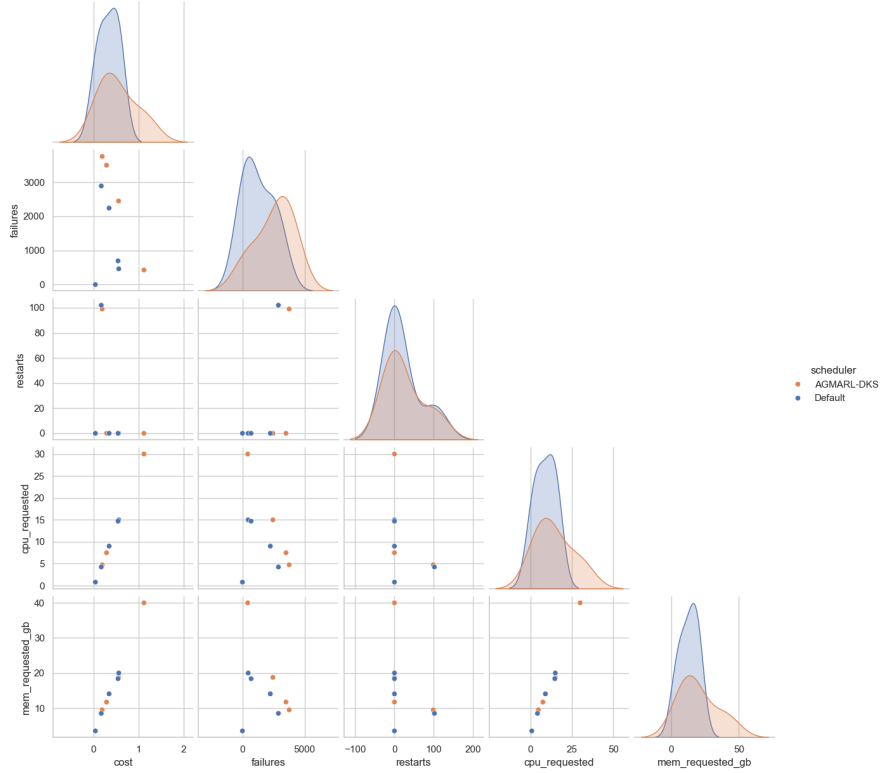


**Fig. 13:** Pairplot of performance metrics for Scenario 1 (Cascading Resource Pressure). The AGMARL-DKS scheduler (orange) demonstrates a tighter clustering in the desirable low-cost, low-failure region compared to the default scheduler (blue).

scheduler manifest a failure in this scheduler to handle the trade-off between cost and failure. The scheduler delivers inconsistent performance under these unstable conditions across both of our measurement metrics. On the other hand, the AGMARL-DKS scheduler has shown a much higher degree of control in these conditions by successfully decoupling its objectives. The AGMARL-DKS scheduler achieves its main success by stopping issues of stability from resulting in expensive placement decisions, although it cannot stop injected failures. This is made manifest in the coupling between failures and cost. In the upper right panel, we can see that the cost of decisions made by the AGMARL-DKS agent stays tightly bunched around 0 even when the number of failures scales to the thousands. On the other hand, there is an obvious positive correlation between failure and cost for the Default scheduler, with high-failure states frequently leading to high-cost, inefficient placement. The performance of the agent’s lexicographical policy demonstrates that its sole focus on stability within a more challenging environment does not represent the optimal strategy of implementing over-provisioning to mitigate such issues. Rather, its learned, GNN-informed value function has enabled the agent to learn to find better, more optimal solutions that are

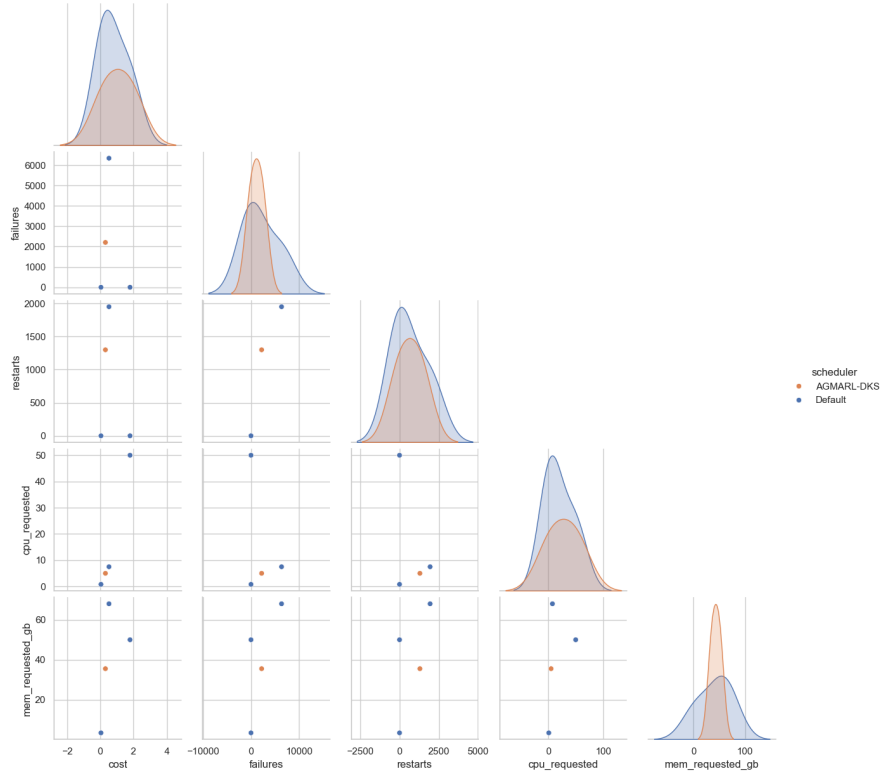


**Fig. 14:** Pairplot of performance metrics for Scenario 2 (Volatile Churn). Even in a chaotic environment, the AGMARL-DKS scheduler (orange) maintains a superior trade-off profile, achieving lower costs and more predictable outcomes than the default scheduler (blue).

both stable and low-cost across a variety of different, more adverse conditions. This ability to find better solutions along the Pareto frontier in a variety of different conditions also serves to validate the key architectural decisions of the AGMARL-DKS framework.

## 7 Conclusion and Future Work

In our paper, we present AGMARL-DKS, a multi-agent reinforcement learning framework that tackles the complex, multi-objective pod scheduling problem in large-scale, dynamic Kubernetes clusters. Traditional schedulers often struggle to optimally balance competing objectives like fault tolerance, resource utilisation, and cost efficiency. AGMARL-DKS addresses these challenges by leveraging a novel combination of a multi-agent system, a stress-aware lexicographical policy for objective prioritisation, and Graph Neural Networks (GNNs) to give agents global cluster context for decentralised decision-making. The production-grade Google Kubernetes Engine (GKE)

cluster evaluation supports the superior performance of AGMARL-DKS versus the standard Kubernetes scheduler across many different test scenarios. AGMARL-DKS displayed intelligent packing behaviour in resource-centric situations by filling select nodes with resource-intensive batch jobs while keeping other nodes partially free. Under volatile conditions with high churn rates and fault injections, our system demonstrated robustness by limiting admission of unstable pods strategically to maintain system stability, thereby enabling faster service delivery of high-priority traffic compared to the default scheduler.

The AGMARL-DKS approach is a comprehensive and effective method for addressing the complex problem of container orchestration in Kubernetes. It overcomes various challenges of modern-day cloud-native applications by successfully integrating the lexicographical multi-objective optimisation method with the advanced multi-agent reinforcement learning framework. The experimental results, including the comparison with four state-of-the-art approaches and the A/B test, show the superiority of AGMARL-DKS in terms of success rate, adaptation speed, system resilience, cost savings, and more. This study can be extended further by applying the proposed methodology to other critical areas of Kubernetes management, such as smarter auto-scaling and network policy optimization. The ultimate objective is to incorporate this advanced scheduling intelligence into production environments allowing multiple operators to leverage it in various operational scenarios.

## 8 Acknowledgment

We would like to thank Dr Artie Basukoski for proofreading the manuscript.

## References

1. Carrión C (2022) Kubernetes as a standard container orchestrator - A bibliometric analysis. *Journal of Grid Computing* 20(4). <https://doi.org/10.1007/s10723-022-09629-8>
2. Truyen E, Van Landuyt D, Preuveneers D, Lagaisse B, Joosen W (2019) A comprehensive feature comparison study of Open-Source Container Orchestration Frameworks. *Applied Sciences* 9(5):931. <https://doi.org/10.3390/app9050931>
3. <https://kubernetes.io/docs/concepts/workloads/pods/>
4. Senjab K, Abbas S, Ahmed N, Khan AUR (2023) A survey of Kubernetes scheduling algorithms. *Journal of Cloud Computing Advances Systems and Applications* 12(1). <https://doi.org/10.1186/s13677-023-00471-1>
5. Zhou N, Zhou H, Hoppe D (2022) Containerization for High performance Computing Systems: Survey and Prospects. *IEEE Transactions on Software Engineering* 49(4):2722–2740. <https://doi.org/10.1109/tse.2022.3229221>
6. Marchese A, Tomarchio O (2025) Enhancing the Kubernetes Platform with a Load-Aware Orchestration Strategy. *SN Computer Science* 6(3). <https://doi.org/10.1007/s42979-025-03712-z>
7. Rejiba Z, Chamanara J (2022) Custom Scheduling in Kubernetes: A survey on common problems and solution approaches. *ACM Computing Surveys* 55(7):1–37. <https://doi.org/10.1145/3544788>

8. Jian Z, Xie X, Fang Y, Jiang Y, Lu Y, Dash A, Li T, Wang G (2023) DRS: A deep reinforcement learning enhanced Kubernetes scheduler for microservice-based system. *Software Practice and Experience* 54(10):2102–2126. <https://doi.org/10.1002/spe.3284>
9. Farid M, Lim HS, Lee CP, Zarakovitis CC, Chien SF (2025) Optimizing Kubernetes with Multi-Objective Scheduling Algorithms: A 5G Perspective. *Computers* 14(9):390. <https://doi.org/10.3390/computers14090390>
10. Carrión C (2022b) Kubernetes scheduling: taxonomy, ongoing issues and challenges. *ACM Computing Surveys* 55(7):1–37. <https://doi.org/10.1145/3539606>
11. Di Cicco N, Poltronieri F, Santos J, Zaccarini M, Tortonesi M, Stefanelli C, De Turck F (2024) Multi-Objective Scheduling and Resource Allocation of Kubernetes Replicas Across the Compute Continuum. 2024 20th International Conference on Network and Service Management (CNSM) :1–9. <https://doi.org/10.23919/cnsm62983.2024.10814307>
12. Wang X, Zhao K, Qin B (2023c) Optimization of Task-Scheduling strategy in edge kubernetes clusters based on deep reinforcement learning. *Mathematics* 11(20):4269. <https://doi.org/10.3390/math11204269>
13. Jayanetti A, Halgamuge S, Buyya R (2024b) Reinforcement Learning based Workflow Scheduling in Cloud and Edge Computing Environments: A Taxonomy, Review and Future Directions. *arXiv (Cornell University)*. <https://doi.org/10.48550/arxiv.2408.02938>
14. Park J, Bakhtiyar S, Park J (2021b) ScheduleNet: Learn to solve multi-agent scheduling problems with reinforcement learning. *arXiv (Cornell University)*. <https://doi.org/10.48550/arxiv.2106.03051>
15. Aina KO, Ha S (2025b) Deep reinforcement learning for Multi-Agent coordination. In: *arXiv.org*. <https://arxiv.org/abs/2510.03592v1>
16. Li, Y., Zhong, W. & Wu, Y. Multi-objective flexible job-shop scheduling via graph attention network and reinforcement learning. *J Supercomput* 81, 293 (2025). <https://doi.org/10.1007/s11227-024-06741-2>
17. Gaon M, Brafman R I (2019b) Reinforcement Learning with Non-Markovian Rewards. In: *arXiv.org*. <https://arxiv.org/abs/1912.02552>
18. Zhou, G., Tian, W., Buyya, R. et al. Deep reinforcement learning-based methods for resource scheduling in cloud computing: a review and future directions. *Artif Intell Rev* 57, 124 (2024). <https://doi.org/10.1007/s10462-024-10756-9>
19. Jalali Khalil Abadi, Z., Mansouri, N. & Javidi, M.M. Deep reinforcement learning-based scheduling in distributed systems: a critical review. *Knowl Inf Syst* 66, 5709–5782 (2024). <https://doi.org/10.1007/s10115-024-02167-7>
20. Kim YG, Wu C-J (2020) AutoScale: Energy Efficiency Optimization for Stochastic Edge Inference Using Reinforcement Learning. 2020 53rd Annual IEEE/ACM International Symposium on Microarchitecture (MICRO) :1082–1096. <https://doi.org/10.1109/micro50266.2020.00090>
21. Rothman J, Chamanara J (2023) An RL-Based Model for Optimized Kubernetes Scheduling. 2023 IEEE 31st International Conference on Network Protocols (ICNP) :1–6. <https://doi.org/10.1109/icnp59255.2023.10355623>
22. Shukla, J.: Comparative study of RL algorithms for resource optimization scheduling in Kubernetes. MSc Thesis, National College of Ireland (2024). Available at: <https://norma.ncirl.ie/8056/>
23. Anouar, H., Hatim, H., Zineb, E.A. (2025). Proposing a Theoretical Energy Aware Framework for Kubernetes Scheduling Using Reinforcement Learning. In: Ezziyyani, M., Kacprzyk, J., Balas, V.E. (eds) *International Conference on Advanced Intelligent Systems for Sustainable Development (AI2SD 2024)*. AI2SD 2024. Lecture Notes in Networks and Systems, vol 1403. Springer, Cham. <https://doi.org/10.1007/978-3-031-91337-2-75>

24. Liang J, Miao H, Li K, Tan J, Wang X, Luo R, Jiang Y (2025) A review of Multi-Agent Reinforcement Learning Algorithms. *Electronics* 14(4):820. <https://doi.org/10.3390/electronics14040820>
25. Danino T, Ben-Shimol Y, Greenberg S (2023) Container allocation in cloud environment using Multi-Agent deep reinforcement learning. *Electronics* 12(12):2614. <https://doi.org/10.3390/electronics12122614>
26. Soulé J, Jamont J-P, Occello M, Traonouez L-M, Théron P (2025) Streamlining Resilient Kubernetes Autoscaling with Multi-Agent Systems via an Automated Online Design Framework. In: arXiv.org. <https://arxiv.org/abs/2505.21559v1>
27. Amato C (2024) An introduction to centralized training for decentralized execution in cooperative Multi-Agent Reinforcement learning. In: arXiv.org. <https://arxiv.org/abs/2409.03052v1>
28. Xu, L., Chen, W., Liu, X., Chen, YY. (2023). MADDPG: Multi-agent Deep Deterministic Policy Gradient Algorithm for Formation Elliptical Encirclement and Collision Avoidance. In: Ren, Z., Wang, M., Hua, Y. (eds) Proceedings of 2021 5th Chinese Conference on Swarm Intelligence and Cooperative Control. Lecture Notes in Electrical Engineering, vol 934. Springer, Singapore. <https://doi.org/10.1007/978-981-19-3998-3-24>
29. Wang, Y., Wu, F. (2021). Policy Adaptive Multi-agent Deep Deterministic Policy Gradient. In: Uchiya, T., Bai, Q., Marsá Maestre, I. (eds) PRIMA 2020: Principles and Practice of Multi-Agent Systems. PRIMA 2020. Lecture Notes in Computer Science(), vol 12568. Springer, Cham. <https://doi.org/10.1007/978-3-030-69322-0-11>
30. Lahande P, Kaveri P, Saini J (2023) Reinforcement learning for reducing the interruptions and increasing fault tolerance in the cloud environment. *Informatics* 10(3):64. <https://doi.org/10.3390/informatics10030064>
31. Xu Z, Gong Y, Zhou Y, Bao Q, Qian W (2024) Enhancing Kubernetes Automated Scheduling with Deep Learning and Reinforcement Techniques for Large-Scale Cloud Computing Optimization. In: arXiv.org. <https://arxiv.org/abs/2403.07905v1>
32. Kallel A, Rezik M, Khemakhem M (2024) DRL4HFC: Deep Reinforcement Learning for Container-Based Scheduling in Hybrid FOG/Cloud System. Proceedings of the 14th International Conference on Agents and Artificial Intelligence :231–242. <https://doi.org/10.5220/0012356800003636>
33. Krishnan, R., Durairaj, S. Reliability and performance of resource efficiency in dynamic optimization scheduling using multi-agent microservice cloud-fog on IoT applications. *Computing* 106, 3837–3878 (2024). <https://doi.org/10.1007/s00607-024-01301-1>
34. Yang Y, Ren F, Zhang M (2024) A decentralized Multiagent-Based task scheduling framework for handling uncertain events in fog computing. In: arXiv.org. <https://arxiv.org/abs/2401.02219v1>
35. Gasior, J., Seredyński, F. (2015). A Decentralized Multi-agent Approach to Job Scheduling in Cloud Environment. In: Angelov, P., et al. Intelligent Systems'2014. Advances in Intelligent Systems and Computing, vol 322. Springer, Cham. <https://doi.org/10.1007/978-3-319-11313-5-36>
36. Gao X, Liu R, Kaushik A (2020) Hierarchical Multi-Agent optimization for resource allocation in cloud computing. *IEEE Transactions on Parallel and Distributed Systems* 32(3):692–707. <https://doi.org/10.1109/tpds.2020.3030920>
37. Pan J, Wei Y (2024) A deep reinforcement learning-based scheduling framework for real-time workflows in the cloud environment. *Expert Systems With Applications* 255:124845. <https://doi.org/10.1016/j.eswa.2024.124845>
38. Lera, I., Guerrero, C. Multi-objective application placement in fog computing using graph neural network-based reinforcement learning. *J Supercomput* 80, 27073–27094 (2024). <https://doi.org/10.1007/s11227-024-06439-5>

39. Oroojlooy, A., Hajinezhad, D. A review of cooperative multi-agent deep reinforcement learning. *Appl Intell* 53, 13677–13722 (2023). <https://doi.org/10.1007/s10489-022-04105-y>
40. He, K., Doshi, P. & Banerjee, B. Modeling and reinforcement learning in partially observable many-agent systems. *Auton Agent Multi-Agent Syst* 38, 12 (2024). <https://doi.org/10.1007/s10458-024-09640-1>
41. Lee D, Lim H-D, Kim DW (2023) Continuous-Time distributed dynamic programming for networked Multi-Agent Markov decision processes. In: arXiv.org. <https://arxiv.org/abs/2307.16706v7>
42. Chen H-C, Li S-A, Chang T-H, Feng H-M, Chen Y-C (2024) Hybrid centralized training and decentralized execution reinforcement learning in Multi-Agent Path-Finding simulations. *Applied Sciences* 14(10):3960. <https://doi.org/10.3390/app14103960>
43. Liang F, Qian C, Yu W, Griffith D, Golmie N (2022) Survey of Graph Neural Networks and Applications. *Wireless Communications and Mobile Computing* 2022:1–18. <https://doi.org/10.1155/2022/9261537>
44. Bonjour, T., Haliem, M., Alsalem, A., Thomas, S., Li, H., Aggarwal, V., Kejriwal, M., Bhargava, B.: Decision making in monopoly using a hybrid deep reinforcement learning approach. *IEEE Transactions on Emerging Topics in Computational Intelligence*. 6, 1335–1344 (2022). <https://doi.org/10.1109/tetci.2022.3166555>.
45. Sun Y, Ma L, Liu Y, Wang S, Zhang J, Zheng Y, Yun H, Lei L, Kang Y, Ye L (2022) Lexicographic Multi-Objective Reinforcement learning. *Proceedings of the Thirty-First International Conference on Artificial Intelligence*. <https://doi.org/10.24963/ijcai.2022/476>
46. Yang B, Gao L, Zhou F, Yao H, Fu Y, Sun Z, Tian F, Ren H (2025) A coordination optimization framework for Multi-Agent reinforcement learning based on reward redistribution and experience reutilization. *Electronics* 14(12):2361. <https://doi.org/10.3390/electronics14122361>
47. Sun Q, Yao Y, Yi P, Hu Y, Yang Z, Yang G, Zhou X (2022a) Learning controlled and targeted communication with the centralized critic for the multi-agent system. *Applied Intelligence* 53(12):14819–14837. <https://doi.org/10.1007/s10489-022-04225-5>
48. Li T, Shi D, Jin S, Wang Z, Yang H, Chen Y (2024a) Multi-Agent hierarchical graph Attention Actor–Critic reinforcement learning. *Entropy* 27(1):4. <https://doi.org/10.3390/e27010004>
49. Xiong F, Zhang Y, Kuang X, He L, Han X (2024) Multi-agent dual actor-critic framework for reinforcement learning navigation. *Applied Intelligence* 55(2). <https://doi.org/10.1007/s10489-024-05933-w>
50. Kim C (2025) Classification-Based Q-Value estimation for continuous Actor-Critic reinforcement learning. *Symmetry* 17(5):638. <https://doi.org/10.3390/sym17050638>
51. Hamilton WL, Ying Z, Leskovec J (2017) Inductive representation learning on large graphs. *Neural Information Processing Systems* 30:1024–1034
52. Dornaika, F., Bi, J. & Charafeddine, J. Leveraging Graph Convolutional Networks for Semi-supervised Learning in Multi-view Non-graph Data. *Cogn Comput* 17, 73 (2025). <https://doi.org/10.1007/s12559-025-10428-y>
53. Konda VR, Tsitsiklis JN (2002) Actor-critic algorithms
54. Lu, C., Bao, Q., Xia, S. et al. Centralized reinforcement learning for multi-agent cooperative environments. *Evol. Intel.* 17, 267–273 (2024). <https://doi.org/10.1007/s12065-022-00703-4>
55. Letsios D, Mistry M, Misener R (2020) Exact lexicographic scheduling and approximate rescheduling. *European Journal of Operational Research* 290(2):469–478. <https://doi.org/10.1016/j.ejor.2020.08.032>

56. Bubboloni D, Gori M (2020) Breaking ties in collective decision-making. *Decisions in Economics and Finance* 44(1):411–457. <https://doi.org/10.1007/s10203-020-00294-8>
57. Xu X, Liu K, Dai P, Jin F, Ren H, Zhan C, Guo S (2022b) Joint task offloading and resource optimization in NOMA-based vehicular edge computing: A game-theoretic DRL approach. *Journal of Systems Architecture* 134:102780. <https://doi.org/10.1016/j.sysarc.2022.102780>
58. Lowe R, Wu Y, Tamar A, Harb J, Abbeel OP, Mordatch I (2017b) Multi-Agent Actor-Critic for mixed Cooperative-Competitive environments. *arXiv (Cornell University)* 30:6379–6390
59. Mnih V, Kavukcuoglu K, Silver D, Rusu AA, Veness J, Bellemare MG, Graves A, Riedmiller M, Fidjeland AK, Ostrovski G, Petersen S, Beattie C, Sadik A, Antonoglou I, King H, Kumaran D, Wierstra D, Legg S, Hassabis D (2015) Human-level control through deep reinforcement learning. *Nature* 518(7540):529–533. <https://doi.org/10.1038/nature14236>
60. David Silver, Guy Lever, Nicolas Heess, Thomas Degris, Daan Wierstra, and Martin Riedmiller. 2014. Deterministic policy gradient algorithms. In *Proceedings of the 31st International Conference on International Conference on Machine Learning - Volume 32 (ICML'14)*. JMLR.org, 1–387–1–395.
61. Zhang S, Sutton RS (2017) A deeper look at experience replay. In: *arXiv.org*. <https://arxiv.org/abs/1712.01275v3>
62. Sehgal A, La HM, Louis SJ, Nguyen H (2019) Deep Reinforcement Learning using Genetic Algorithm for Parameter Optimization. In: *arXiv.org*. <https://arxiv.org/abs/1905.04100v1>
63. Gu S, Lillicrap T, Ghahramani Z, Turner RE, Schölkopf B, Levine S (2017) Interpolated Policy gradient: Merging On-Policy and Off-Policy gradient estimation for deep reinforcement learning. In: *arXiv.org*. <https://arxiv.org/abs/1706.00387v1>
64. Google Cloud, "Google Kubernetes Engine (GKE)," Google Cloud, [Online]. Available: <https://cloud.google.com/kubernetes-engine>.